NVE

Jernbaneverket

Statens vegvesen

Natural Hazards project: Work Package 6
- Quick clay

Back-analyses of run-out for Norwegian quick-clay landslides

46
2013

R A P P O R T

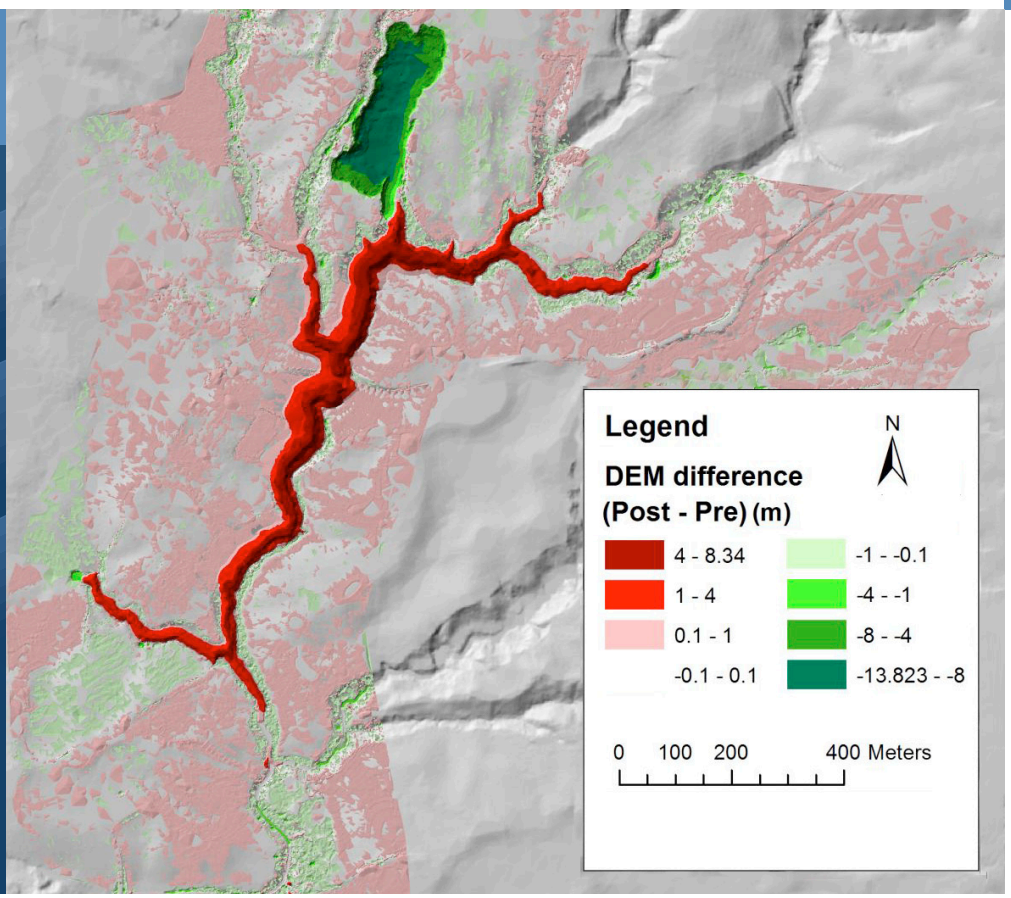

NIFS
NATURFARE
INFRASTRUKTUR - FLOM - SKRED

Natural Hazards project: Work Package 6 - Quick clay

Back-analyses of run-out for Norwegian quick-clay landslides

Norwegian Water Resources and Energy Directorate in collaboration with Norwegian Public Roads Administration and Norwegian National Railways Administration

2013

Report nr. 46/2013
Back-analyses of run-out for Norwegian quick-clay landslides
Publisher: Norwegian Water Resources and Energy Directorate in collaboration with Norwegian Public Roads Administration and Norwegian National Railways Administration
Prepared by: Norwegian Geotechnical Institute (NGI)
Authors: Dieter Issler, José Mauricio Cepeda, Byron Quan Luna and Vittoria Venditti (ICG/ Università di Bologna)
Date: 30.11.2012
ISBN: 978-82-410-0917-4

Preface: Norwegian Public Roads Administration (NPRA), Norwegian Energy and Water Resources (NVE) and Norwegian National Railways Administration (NNRA) have initiated a National R&D project (2012-2015) called *Natural Hazards – Infrastructure for flood and slides.* The estimated budget for the project is 42 Million Norwegian Kroners. Quick clay is one of the seven work packages of the project. More information about the project can be obtained at www.naturfare.no

As a part of the on-going collaboration, NGI has been given a task to do a pre-study on the mobility of landslides in quick clays. The report presents results from numerical simulations carried-out on a few well documented quick clay landslides with BING, DAN3D and MssMov2D.

Keywords: Quick-clay, simulation, Q-Bing, BING, DAN3D, MassMov2D

NGI Rapport / Report

NIFS-N1 Q-Bing — Utløpsmodell for kvikk-leireskred

Back-analyses of run-out for Norwegian quick-clay landslides

20120753-01-R
30 November 2012
Revision: 0

Main office:
PO Box 3930 Ullevål Stadion
NO-0806 Oslo
Norway

Trondheim office:
PO Box 1230 Sluppen
NO-7462 Trondheim
Norway

T (+47) 22 02 30 00
F (+47) 22 23 04 48

BIC No. DNBANOKK
IBAN NO26 5096 0501 281
Company No.
958 254 318 MVA

ngi@ngi.no
www.ngi.no

Project

Project title:	NIFS-N1 Q-Bing — Utløpsmodell for kvik-leireskred
Document title:	Back-analyses of run-out for Norwegian quick-clay landslides
Document No.:	20120753-01-R
Date:	30 November 2012
Revision/Rev. date:	0

Client

Client:	Statens Vegvesen, Veidirektoratet
Client's contact person:	Vikas Thakur
Contract reference:	Contract, revised 2012-08-20

For NGI

Project manager:	Dieter Issler
Prepared by:	Dieter Issler, José Mauricio Cepeda, Byron Quan Luna and Vittoria Venditti (ICG/ Università di Bologna)
Reviewed by:	Kjell Karlsrud

Summary

The objective of this report is to assess the degree to which existing flow models, developed for other types of gravity mass flows, might be used for quick-clay slides. To this end, data from the 2012 Byneset slide (subaerial), the 1996 Finneidfjord slide (mostly subaqueous) and the 1978 Rissa slide (transition from subaerial to subaqueous) were collected and analyzed so as to be used as input to, and judge for, numerical simulations. The main models used in this back-calculation are BING, a quasi-2D code based on visco-plastic rheology of the Herschel–Bulkley type, and DAN3D, a quasi-3D code with a choice of rheologies (or bed friction laws) like purely frictional, purely plastic, Newtonian, Bingham and Voellmy. A first exploratory simulation of the Byneset slide with MassMov2D was also carried out.

Summary (cont.)

It was found that different numerical codes implementing the same rheology may give rather different results for the same input parameters and that the tested models required ad hoc adjustments for dealing with subaqueous flow (DAN3D, MassMov2D) or with the transition from subaerial to subaqueous conditions (BING). A source of substantial error in all three models under subaqueous conditions is the lack of a model capturing the effects of hydrodynamic drag.

None of the models succeeded in simulating at least one of the test cases satisfactorily with the values of the resistance parameters (yield strength, viscosity or consistency) suggested by geotechnical investigations. It is suggested that this is not the result of numerical problems, but of the inadequacy of representing a quick-clay slide as a simple, homogeneous visco-plastic fluid (or possibly some other fluid). As the tested models are of today, they do not seem to be generally applicable in consulting projects involving quick-clay slides.

A future model of quick-clay slides should therefore take into account the multi-layer structure of most quick-clay slides with non-sensitive material riding piggy-back on the quick-clay layer. Furthermore, it appears necessary that the model have the capacity of computing, or letting the user specify, a retrogressive release sequence. In view of applications to subaqueous slides, it is highly desirable to include buoyancy and drag effects.

Contents

1 Introduction

Quick-clay slides in sensitive marine clay deposits are a major natural hazard in coastal areas of Alaska, eastern Canada, Scandinavia and northern Russia. Alone in Norway, over 1000 persons have died in such slides, and even as recently as 1893, the Verdal slide killed 116 persons (Furseth, 2006; Walberg, 1993). Since the 1950s, focused research has uncovered the key mechanisms by which originally over-consolidated, stable clay layers become highly sensitive, leading to instability and catastrophic slides; for a brief review, see e.g. (L'Heureux, 2012b). Understanding these mechanisms has made it possible to identify areas prone to quick-clay slides, and a large-scale project is under way in Norway to map all parts of the country where quick clay may be found.

The Norwegian procedures for mapping of areas prone for quick-clay slides so far are limited to identifying quick-clay deposits that may become unstable if a suitable triggering event occurs. In many cases, however, it is also necessary to assess the extent of the area that could be affected by the flow of the landslide masses. For all other types of gravity mass movements, like debris flows, rock and snow avalanches, analysis of the potential run-out area is the most important aspect of the mapping because settlements are not usually located in the steep potential release areas. Quick-clay slides may originate from gently sloped areas that otherwise may be desirable for construction purposes. Additionally, in many cases erosion by a river is the relevant trigger and the slide masses follow the course of the river. Therefore, the mapping of the potential run-out areas has been less of a concern for quick-clay slides than for other types of slides. Nevertheless, there are also numerous cases where inhabited areas may be affected by a quick-clay slide, and the need for modeling the potential run-out areas has been increasingly felt in recent years.

At present, no specific model for calculating quick-clay slide run-out is available. A rule of thumb used in Norway says that all downstream areas for which the average slope from the top of the potential release area is more than 1/15 should be considered endangered. The coordinated NGI projects 20120167 "SP1.2012.07 Q-Bing" and 20120753 "NIFS-N1 Q-Bing – Utløpsmodell for kvikkleireskred" aim at developing a dynamical model that is adapted to the specific properties of quick-clay slides. The report by L'Heureux (2012b) analyzes the key morphological and geotechnical properties of quick-clay slides on the basis of a database containing approximately 40 well-described events. The objective of the present report is to assess to which degree models developed for other types of landslides succeed in simulating quick-clay slides or in which respect they fail. Information from both studies will be useful in the design of a specific run-out model for quick-clay slides.

To this purpose, three well-documented recent Norwegian quick-clay landslides were back-calculated, namely the ones at Rissa in 1978—the largest to have struck Norway in recent times—, the 1996 Finneidfjord slide, and the 2012 event at Byneset. In all three cases, the slide deposits could be mapped with good precision, some velocity estimates are available for the Rissa slide, and geotechnical

investigations have been performed (or will be completed soon in the case of Byneset). The characteristics of these slides and the available data are described in more detail in Section 2.

The choice among the large number of numerical models developed for other landslide types or snow avalanches was largely dictated by practical reasons (time and funding constraints, availability of the models at NGI, previous experience in their use), but also by considering how close their rheological basis may match the behavior of quick clay (for more details on the models, see Section 3):

- BING (Imran et al., 2001) is a quasi-2D numerical model developed for mudflows on the basis of the Herschel–Bulkley rheology. It has been used in several NGI projects involving subaqueous debris flows. Several variants of the original model were developed in connection with the EU project COSTA and the study of the Storegga slide in the framework of the Ormen Lange project (De Blasio et al., 2003, 2004, 2005). One of the authors recently applied the original BING code to the 1978 Rissa slide (L'Heureux et al., 2011).
- DAN3D (McDougall and Hungr, 2004; McDougall, 2006) is a quasi-3D model. It gives the user a choice of different bed-friction laws, ranging from Coulomb to Voellmy and Bingham. It has been widely used since its publication and was also tested in a research project at NGI (Gauer and Cepeda, 2007). Combined with BING in this study, it offers the possibility to assess the importance of including the transversal dimension while the rheology is kept the same, and to compare different rheological assumptions in the same numerical framework.
- MassMov2D (Beguería et al., 2009) has many features in common with DAN3D, given that it is also a quasi-3D model and offers a similar choice of bed friction laws. It is, however, based on a different numerical approach, i.e., the more traditional Eulerian one instead of Smoothed Particle Hydrodynamics (SPH) employed in DAN3D. Moreover, it is implemented as a script in a open-source geographical information system (GIS).

The approach chosen for the back-calculations consists of the following steps:

1. Digital terrain models (DTMs) of the pre-slide and post-slide topography (and bathymetry in the case of Rissa and Finneidfjord) were obtained. From the difference between them, one obtains the geometry of the failed volume and of the deposit, assuming that bed erosion along the flow path can be neglected.
2. For the simulations with BING, a representative profile line is chosen, again with pre-failure and post-failure topography/bathymetry.
3. Geotechnical data on the slide masses reviewed and transformed into default values for the corresponding model parameters using the relationships reviewed by L'Heureux (2012b).

4. Starting from the default values, the model parameters are varied within physically reasonable bounds until the observed run-out distance, deposit shape and – where available –velocity are reproduced as closely as possible. It has not been attempted to establish objective criteria for the degree of agreement of observation and simulation since this is an exploratory test and the main objective is only to obtain qualitative information on the adequacy of different geometrical and rheological modeling approaches.

The results of these simulations are presented in Section 4, and their significance for the further development of the run-out model for quick-clay slides is discussed in Section 5.

2 Description of test cases

2.1 Essential facts about quick clay and quick-clay slides

The designation "quick clay" refers to clay whose structure collapses completely at remolding and whose shear strength is thereby reduced almost to zero. In Norway, quick clay is defined as clay with sensitivity of 50 or more and fully remolded shear strength of less than 0.4 kPa (NGF, 1974). The sensitivity is the ratio between the undisturbed and the fully remolded undrained shear strengths. The Norwegian marine clays were deposited with a flocculated structure in the sea after the last glaciation about 10,000 years ago. Following the isostatic uplift, the deposits were exposed to surface erosion and weathering (Karlsrud et al., 1984). The clay deposits have then been subjected to leaching, whereby the ion (mainly iron and aluminum) concentration in the pore water has changed. The leaching has been caused by infiltration of water from rain or from underlying permeable soil or rock (due to artesian water pressure). The leaching of the salt in the pore fluid changes the sensitivity of these clays from low (S_t typically 3–6) to high (S_t > 20) (Rosenqvist, 1953, 1966). This is a slow process whose speed strongly depends on local conditions. For this reason, slopes with marine clay deposits that were stable in the past may become quick and unstable in the future.

Rheological tests performed on quick clays yielded the following results, among others (Locat and Demers, 1988; Khaldoun et al., 2009):

- When loaded with a constant shear stress below the yield strength, the clay exhibits high viscosity, typically in the range 10^4–10^5 Pa s, which tends to increase slowly with time. When loaded with a shear stress just above the yield strength, the "card-house" fabric is destroyed in the course of seconds to minutes (remolding) and the yield strength and viscosity drop by several orders of magnitude to very low values.
- The behavior of the *fully remolded* quick clay is well described by the Herschel–Bulkley rheological model, which reads as follows for simple shear, with $\dot{\gamma}$ the shear rate, τ the shear stress, τ_y the yield strength, $n > 0$ the rheological exponent, K (units Pa s^n) the consistency, and sgn(x) the sign of x:

$$\dot{\gamma} = \begin{cases} 0 & \text{for} \quad |\tau| \leq \tau_y, \\ \operatorname{sgn}(\tau)\left(\dfrac{|\tau| - \tau_y}{K}\right)^{1/n} & \text{for} \quad |\tau| > \tau_y. \end{cases} \tag{1}$$

  The value of n is typically between 0.2 and 0.5 and the yield strength less than 0.5 kPa. There is thus pronounced shear-thinning, but many laboratory measurements have only been analyzed in terms of a Bingham fluid, i.e., $n = 1$ was a priori assumed.
- Both the yield strength and the consistency, defined by $= \tau_y \dot{\gamma}_r^{-n}$, diminish approximately exponentially with increasing water content (or liquidity index). Conversely, adding small quantities of salt to the slurry in a critical

range of salt concentration increases these parameters by several orders of magnitude.

- Small-scale chute experiments revealed a non-monotonic decrease of the run-out distance with increasing yield strength (Khaldoun et al., 2009). Those authors attribute this effect to the yield-stress-controlled threshold for dispersion of the released mass. In our opinion, further experiments at somewhat larger scale are required to corroborate this.

Note that the Herschel–Bulkley rheology comprises a number of well-known special cases: For $\tau_y = 0$ and $n = 1$, a Newtonian fluid is recovered. Shear-thinning and shear-thickening (non-plastic) fluids correspond to $\tau_y = 0$, $0 < n < 1$ and $\tau_y = 0$, $n > 1$, respectively. Bingham fluids have $\tau_y > 0$ and $n = 1$. At least for simple shear, the Casson fluid is equivalent to $\tau_y > 0$ and $n = ½$. These relationships are presented graphically in Figure 1.

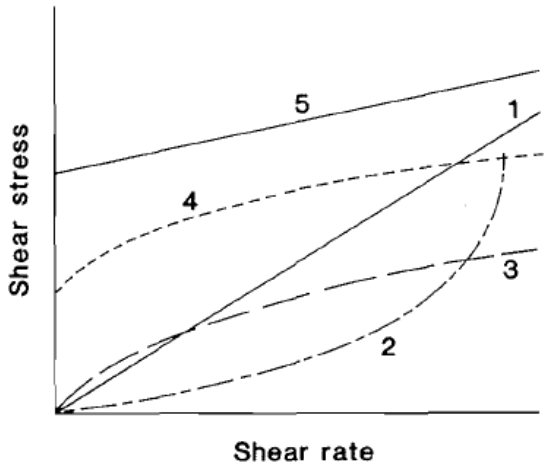

Figure 1. Schematic representation of the relationship between shear rate and shear stress for different types of fluids:
(1) Newtonian,
(2) shear-thickening,
(3) shear-thinning,
(4) Herschel–Bulkley (shear-thinning case, n < 1) and Casson, and
(5) Bingham.

Landslides in sensitive clays fall into four main classes or combinations thereof (see (L'Heureux, 2012b) and references therein for a more detailed discussion): single rotational slides; multiple retrogressive slides; translational progressive landslides; and spreads. In single rotational slides, the slide mass does not liquefy and flow except perhaps for a thin layer at the glide plane; this type of slide can be well described by traditional geotechnical models and is not of concern in the present context. In translational progressive landslides, the upper parts of the slide mass also remain largely intact as a flake or slab, and liquefaction seems limited to a thin shear layer. The run-out distance can be limited (some 10 m in the case of the Bekkelaget landslide) or very long, as in the 1978 Rissa slide (see Sec. 2.2). Multiple retrogressive slides and spreads have in common that the failure proceeds in several distinct stages, each of which renders a portion of the upstream sediments unstable. If the material liquefies and flows out of the crater, a multiple retrogressive slide occurs; in a spread, wedge-like grabens subside between horsts.

Translational progressive landslides and spreads highlight the importance of the top layer of non-sensitive material (clay or sand, gravel and mixtures thereof) that

overlays the sensitive clay. This material is not remolded and its strength exceeds that of the remolded quick clay by several orders of magnitude. It is rafted along when the quick clay liquefies and may break up in the process. The shear stress it exerts on the quick-clay layer is thought to be instrumental in the liquefaction of the latter, which then acts like a lubricating layer. As argued by Khaldoun et al. (2009), a quasi-solid top layer sliding on a liquefied shear layer may achieve longer run-out than a completely liquefying mass that spreads in all directions and quickly becomes too thin to overcome the residual strength of the material.

2.2 The 1978 Rissa landslide, Sør-Trøndelag county

The Rissa landslide took place in April 1978 and is the biggest in Norway during the 20th century with its volume of 5–6 million m^3 from an area of 330.000 m² of sensitive marine clay. The pre-slide topography had a gentle slope of approx. 5° near the shore along the main axis and significantly less farther away from the lake. The vertical extent of the failed volume, H_2 in Figure 2, is 30–35 m, but the total drop height, H_t, attains about 60 m because the landslide took place at the corner of Lake Botn and the slide deposits extend about 1200 m from the shore to a water depth of nearly 30 m, see Figure 3. Upon entering the lake, the Rissa slide masses generated a tsunami with a recorded maximum surface elevation of 6.8 m.

A concise summary of the two-stage landslide event is given by L'Heureux et al. (2012a):

> *At first, an initial slide was triggered due to excavation and stockpiling along the lakeshore. During this initial failure, 70–90 m of the shoreline slid out into the lake, including half of the recently placed earth-fill. The slide edges were 5–6 m high and extended 15–25 m inland. The landslide developed retrogressively in the south-western direction over the next 40 minutes. The sediments completely liquefied during the sliding and the debris literally poured into the lake like streaming water. At this stage the landslide area took the shape of a long and narrow pit open towards the lake (Fig. 3). The length of the sliding area was 450 m, covering an area of 25–30,000 m^2 (6–8 % of the final slide area) (Gregersen, 1981).*
>
> *The main landslide started almost immediately after retrogressive sliding had reached the boundaries of stage 1 (Fig. 3B). At this point large flakes of dry crust (150×200 m) started moving towards the lake, not through the existing gate opening, but in the direction of the terrain slope (see A and B; Fig. 3B). The velocity was initially moderate (flake A; Fig. 3B), of the order of 10–20 km/h, and increased to 30–40 km/h (flake B; Fig. 3B). Houses and farms can be seen floating on the sliding masses on the amateur videos. A series of smaller and retrogressive slides followed over a short period of time. The sliding process propagated to the mountain side where it stopped. The main sliding stage lasted for approximately 5 minutes and covered 92–94% of the total slide area (0.33 km^2). The total volume of mobilized sediment has been estimated in the range of 5–6×10^6 m^3.*

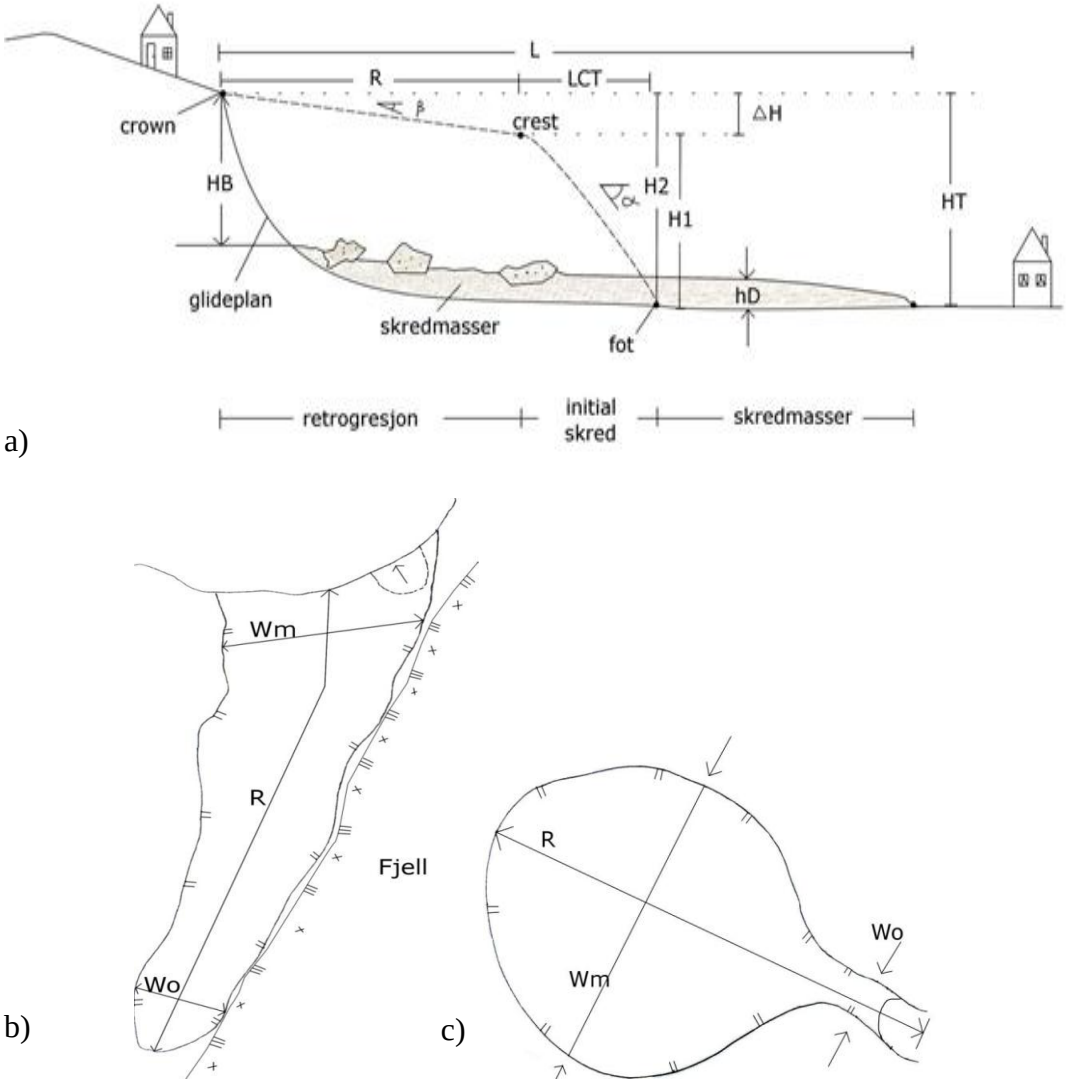

Figure 2. Schematic representations of a landslide and its geometrical characteristics. a) Side view, b) and c) plan view of oblong and pear-shaped slide craters. "Glideplan" is the sliding plane, "crown" and "fot" are the upper and lower intersections of the original terrain surface with the glide plane, "skredmasser" means slide deposit. h_D – deposit depth, H_T – total drop height, H_1 – initial drop height, H_2 – vertical extent of failed volume, ΔH – altitude difference along backslope, H_B – escarpment height, L – total run-out length, L_{CT} – length of foreslope, R – retrogression distance, W_0 – minimum width of the release gate, W_m – maximum width of the release area. From (Natterøy, 2011).

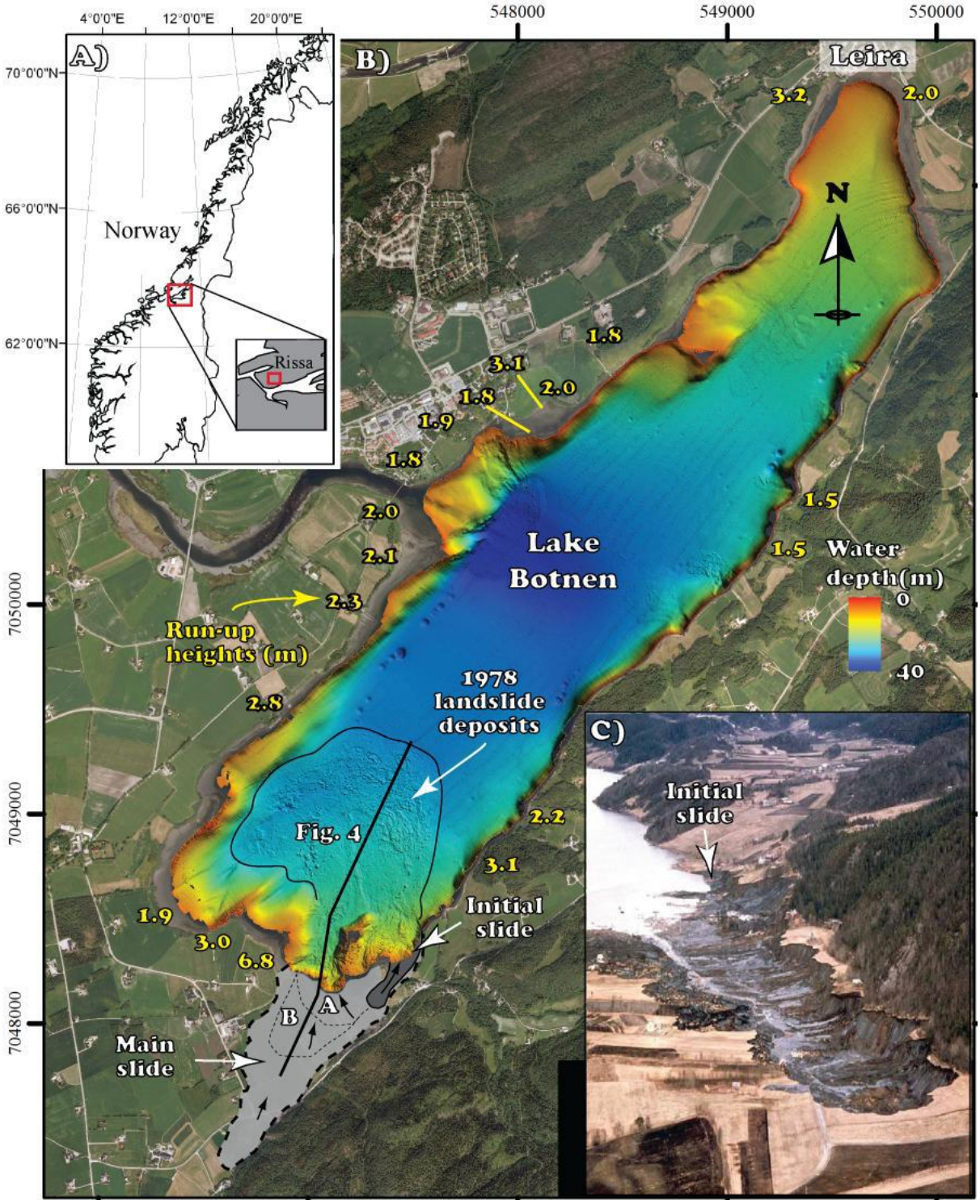

Figure 3. Rissa landslide area: A) Geographic location. B)Map of Lake Botn with color-coded bathymetry, outline of slide deposits and outline of the areas affected by the initial slide (dark grey), the two major flakes A and B, and the subsequent retrogressive slide (light grey). C) Aerial view of the slide pit. From (L'Heureux et al., 2012).

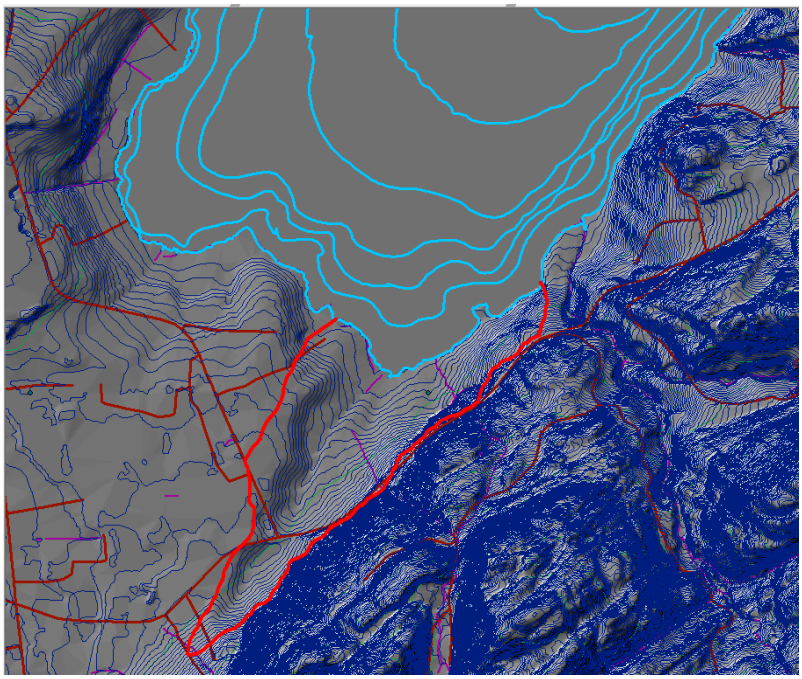

Figure 4. Bathymetry of the Rissa landslide area.

2.3 The 1996 Finneidfjord slide, Hemnes municipality, Nordland county

The Finneidfjord landslide occurred in 1996, mobilizing 1 million m³ of sediments and killing four people. Janbu (1996) reconstructed the sequence of sliding on the basis of then available data as a five-stage event, while later acquired swath bathymetry and seismic data favor a slightly modified interpretation with three main stages (see below). The site investigations revealed also that there has been considerable earlier slide activity near the 1996 site, and there appears to be potential for future slides (Longva et al., 2003). As will be discussed below, only the first stage of the sequence can be considered a quick-clay slide, but its soft deposits may have facilitated longer run-out (and possibly hydroplaning) of the flowing masses in the second stage. It thus represents a purely subaqueous quick-clay slide, in contrast to the completely subaerial Byneset slide (Sec. 2.4 below) and Rissa slide that started on land and ran out in water.

The three main stages can be characterized as follows (Longva et al., 2003):

1. The first detachment occurred along a well-defined horizon characterized by high-amplitude seismic reflections at a typical sub-seabed depth of 6 m. This layer is tentatively interpreted as porous sand layers with interstitial free gas, trapped between silty clay layers (Best et al., 2003). The initial slide (Stage 1) started 1–9 m below sea level at the steepest part of the slope (18°), 50 to 70 m from highway E6 (Figure 6). The sliding material consists of a layer of Holocene sediments. Presumably, the slide progressed retrogressively, widening and encroaching closer on the shore in the process. Retrogression is corroborated by eye witnesses seeing waves, bubbles and swirls moving away from the shore for quite a while, and one

would expect a flake release to trigger a substantial tsunami. As the slide scar widened to as much as 350–450 m, the geometry became that of a "bottle neck" slide with a gate width of about 150 m.

No estimate of the volume of this stage has been found in the literature. For the purpose of initial values for the back-calculations, it is assumed from Figure 6 and Figure 5 that the release width was about 400 m, the length roughly 150 m and its average depth 4 m, giving a volume of 240,000 m^3 (with a large degree of uncertainty).

From swath bathymetry and seismic profiles, the deposits of this stage can be traced where they have not been overflowed by the subsequent, more massive flow stage. In the northern part of the slide deposit area, a sheet of fairly homogeneous material with compression ridges in the distal part contrasts with the hummocky deposits attributed to the later stages. The maximum run-out distance from the Stage 1 slide scar is about 550–600 m, the total drop height about 35–40 m. The deposit area is difficult to determine due to the deposits from Stage 2, but rough estimates suggest it should have been 80,000 m^2 or more. From limited seismic information, an average deposit depth of approximately 2–3 m was inferred. This agrees reasonably well with the estimated release volume.

2. Stage 2 also developed retrogressively to the shore line and beyond. The hummocky deposits cover the sea floor over a distance of up to 800 m from the shore, to a water depth of 40–45 m. The average slope of the deposit area is about 3° (Ilstad et al., 2004). Beyond the main lobe, there is a 100–200 m wide belt of oblong outrunner blocks that stopped on a slope of approx. 1°. The larger ones are 40–70 m in width, 10–20 m in length and 1–2 m in height. The largest block of all (100×50×2 m^3) moved solitarily 1.4 km downslope and was stopped by a moraine ridge. At this stage, parts of the highway E6 and houses approximately 20 m farther inland were swept into the fjord. The most distal portions of the slide material were more competent than the more frontal sediments and plowed into them. Their maximum run-out distance is approx. 370 m from the slide scar (see Figure 5), the total drop height approx. 30 m. The remnants of the road and the house were deposited at most 100 m from the shoreline.

   A rough estimate of the volume of material mobilized during Stage 2 by perusal of Figure 5 and Figure 6, assuming a 300 m wide, 150 m and on average 15–20 m deep release gives a volume of 675–900,000 m^3. The deposits (including outrunner blocks) cover an estimated area of 200–250,000 m^2. Two seismic lines across the deposit indicate a deposit depth of 2–3 m in the lower part and about 5 m in the proximal part, leading to reasonable agreement with the estimated release volume.

3. After stage 2, smaller debris-flow lobes deposited in the eastern part of the slide area marked the end of the instability (Stage 3). Their run-out distance varied between 100 and 250 m, the total drop height is estimated at 25–30 m. The slide volume is tentatively estimated at 30–80,000 m^3. Among other objects, a construction site was swept into the fjord.

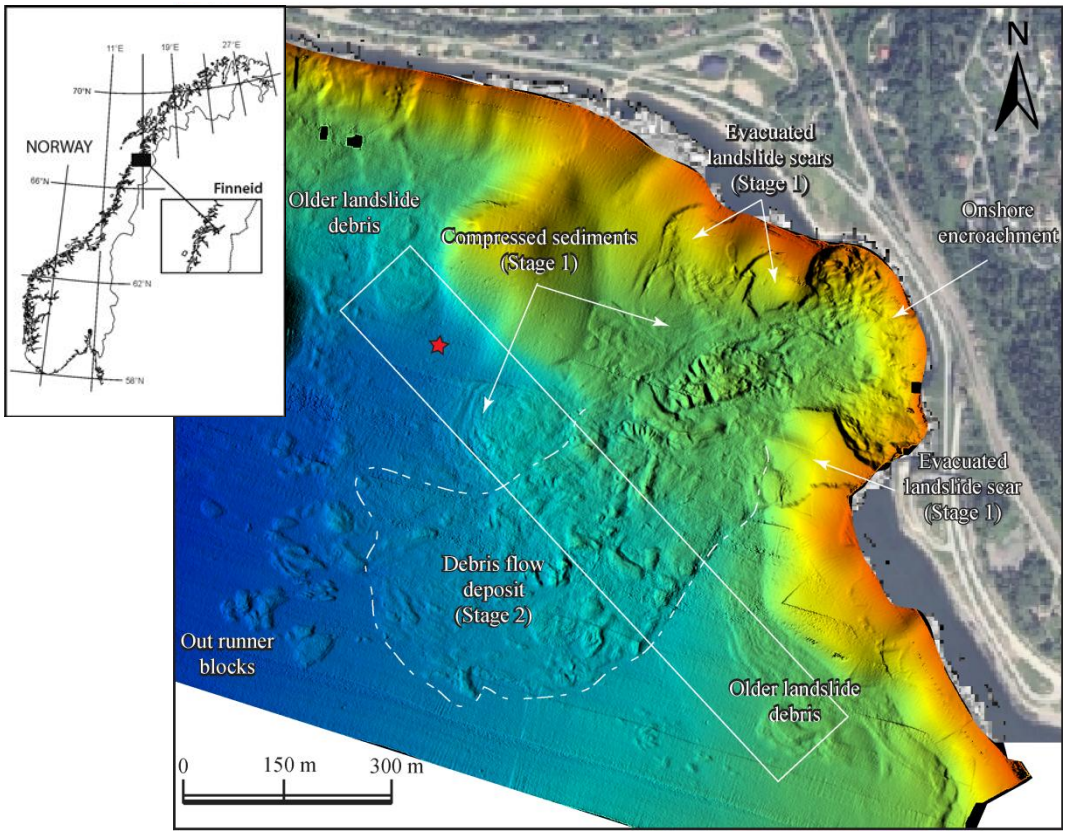

Figure 5. Left: Geographic location of Finneidfjord. From (Longva et al., 2003). Right: Surface morphology of the 1996 slide from high-resolution swath bathymetry with the different stages of the slide as identified by (Longva et al., 2003). The color coding of the bathymetry ranges from 0 m depth (red) to 50 m depth (dark blue). From (Vardy et al., 2012).

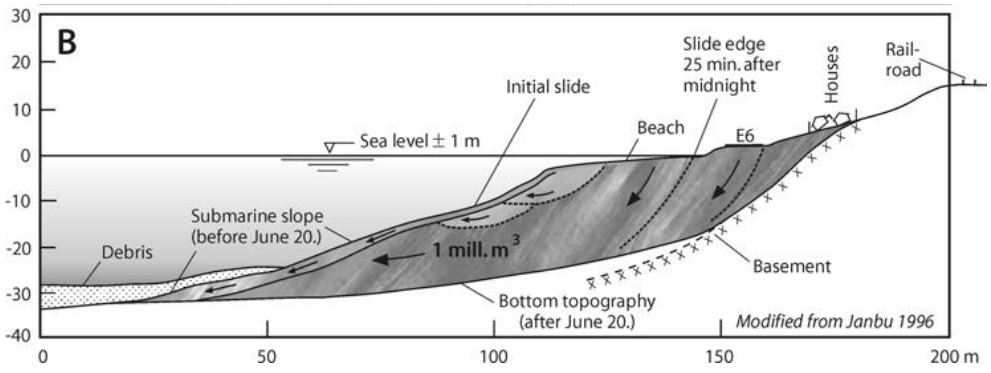

Figure 6. Profile illustrating slide mechanisms with initial detachment within the Holocene succession. The beach was relatively flat before the failure. From (Longva et al., 2003).

The terrain model for Finneidfjord was prepared by merging contours from a 25-m cell bathymetry and 1-m contours on land, both from Norge Digitalt. Before merging these spatial datasets, the land contours were adjusted using the mean sea

level value measured at Bodø (1.64 m), the most representative station in the vicinity of Finneidfjord. The hillshade and 5 m contours of the terrain model are presented in Figure 7. The shape and size of the release area were estimated from (Longva et al., 2003). The outline of, and height distribution within, the source area are presented in Figure 7.

At present, the authors do not have access to pre- and post-slide digital elevation models of sufficient precision to create a DEM for the glide plane and to reconstruct the release volume. (The latter step is made even more difficult by the fact that this was a multi-stage slide and that the horizon of the first stage must be interpolated over most of the area by using data from adjacent areas.) For this reason, the 25 m resolution DEM from the readily available bathymetry was used without accounting for the actual glide plane. (For the simulations with BING, the profile was adjusted manually.)

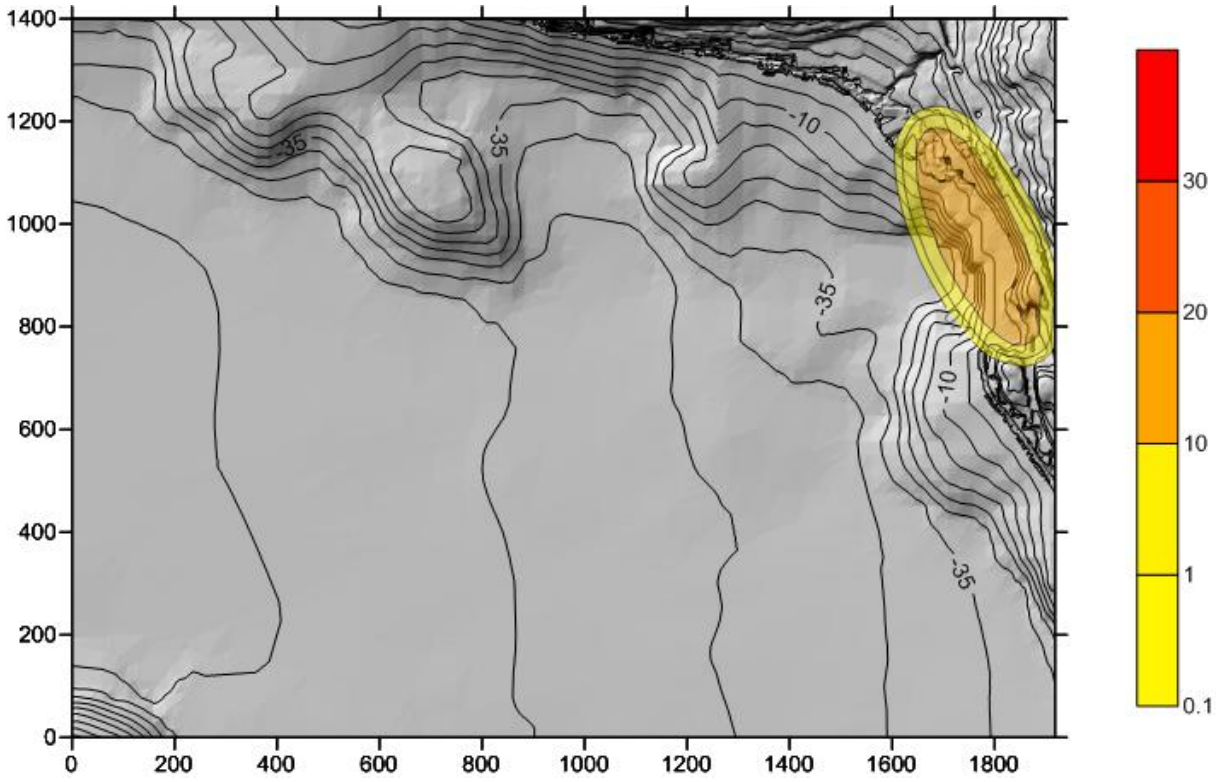

Figure 7. Initial condition for the simulations of the 1996 Finneidfjord slide with DAN3D: spatial distribution of release depth (in meters). Terrain contours are at 5-m intervals.

2.4 The 2012 Byneset slide, Trondheim, Sør-Trøndelag county

During the first hours of 2012, a quick-clay slide with a volume of $2–4 \cdot 10^5$ m^3 was released at Esp in the Byneset area, about 10 km WSW of the city of Trondheim. Near this site, ten quick-clay slides of similar or larger size occurred in the middle of the 19th century over a period of less than 50 years. Some geotechnical

investigations were carried out immediately after the event, but further ground drilling has to wait until the slide masses have consolidated enough to support the weight of the drilling equipment. Remediation work had to be started immediately, however, because the slide masses completely filled the river, damming it as well as several downstream tributaries (Figure 8–Figure 11). Also, access roads to nearby farms were blocked by the deposits.

Assuming that four cores drilled a short distance away from the eastern escarpment are representative for the soil layering in the actual release area, 50–70% of the slide material is quick clay, overlain by non-sensitive clay and/or sand and gravel.

The slide masses evacuated the crater almost completely, as Figure 8 shows. Given the narrow gate and gentle slope along the glide plane, a significant fraction of the quick clay must have been remolded rapidly for this to be possible. Due to low discharge in Brenselbekk (Lyche, 2012), water is not expected to have played an important role in the run-out of the slide.

Figure 8. Bird's eye view of the 2012 Byneset quick-clay slide. The crater in the middle of the image is 8–10 m deep and about 350 m long. Probably it was erosion at the bend of the river that caused the initial failure (IF) that opened the narrow gate through which the main mass of the slide evacuated, following the course of the brook Brenselbekk (indicated by arrow). From (Lyche, 2012).

Terrain models for pre- and post-slide conditions were obtained, respectively, from 1-m contours available from Norge Digitalt, and from the results of a detailed post-slide survey provided by Statens Vegvesen for this project. An analysis of both terrain models allowed estimating the release area and volume, which yielded approximately 32,600 m^2 and 262,000 m^3, respectively, corresponding to a mean depth in the scarp area of about 8 m. The previous estimate of the volume

was approximately 350,000 m^3. Figure 11 shows the release area obtained from the aforementioned procedure, which was used in the DAN3D simulations.

Figure 9. Deposit of the Byneset quick-clay slide completely filling the channel of Brenselbekk. The deposits also dammed tributary brooks. From (Lyche, 2012).

Figure 10. Front of the deposit of the 2012 Byneset slide, approximately 870 m from the gate. The deposit depth is approx. 3 m and increases to approx. 7 m upstream. From (Lyche, 2012).

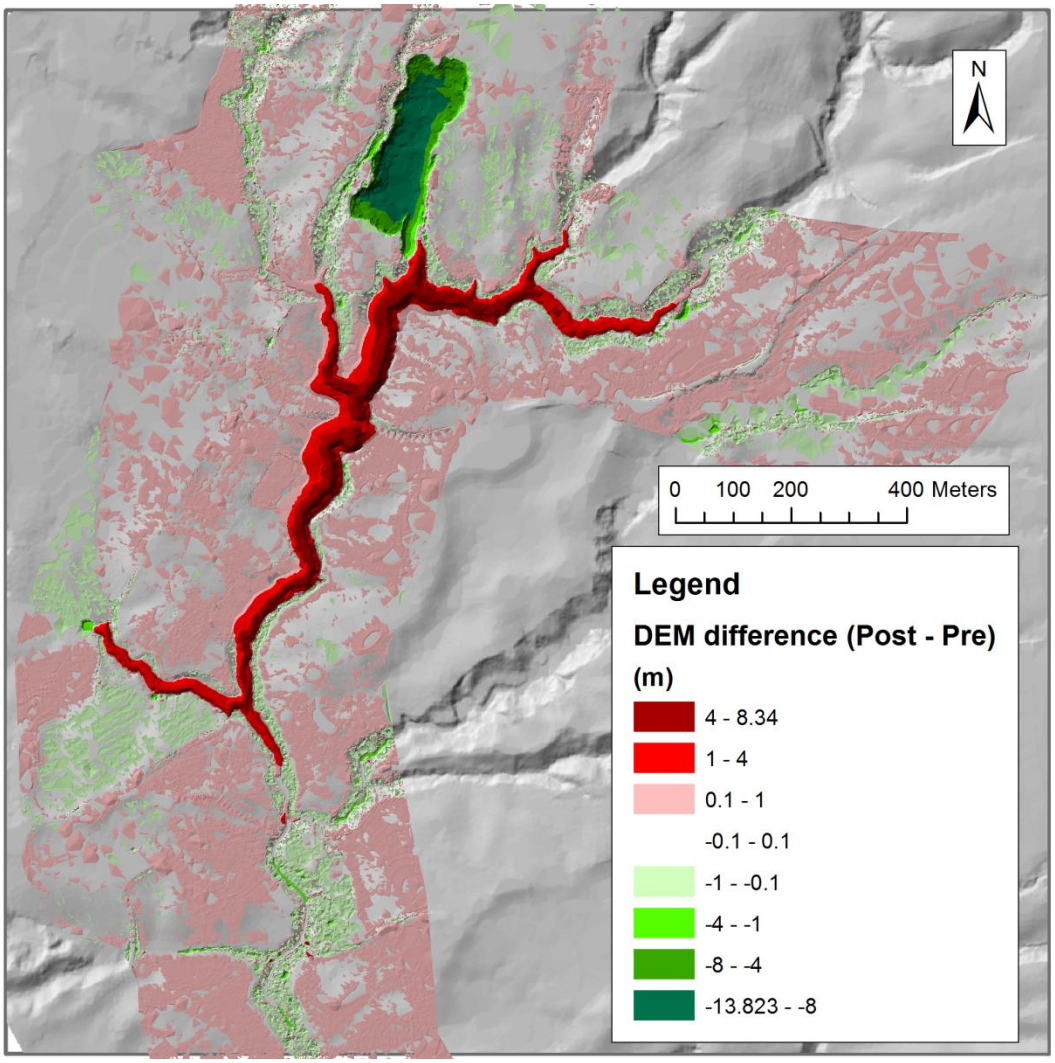

Figure 11. Elevation difference between the post- and pre-landslide digital terrain models for delineating the release area (darker green colours) and the deposit (darker red colours).

The actual distribution of the deposit along the channels was also estimated based on the analysis of the pre- and post-slide DEMs. The deposit is shown as the darker red areas in Figure 11. Note in particular the branching of the flow as well as the upstream run-up to the East of the gate, and also up the western tributaries of the main north-south channel. It is also important to notice that the deposit becomes thinner towards distal end, both along the main channel and along the branches, and that the upstream end of the deposit starts just at the foot of the scarp in the release area. The spatial distribution of the deposit depth shown in Figure 11 is useful for validating the rheological assumptions made by different models because its shape cannot be reproduced simply by tuning friction parameters, as is the case for the run-out distance.

Table 1. Geometrical and geotechnical parameters characterizing the main stage of the 1978 Rissa slide, the initial stage of the 1996 Finneidfjord slide, and the 2012 Byneset slide. For the first two events, data are taken from (Natterøy, 2011). Data on the Byneset slide is from (Lyche, 2012), (NVE, 2012) and (Thakur and Degago, 2012). See Figure 2 for the definition of the geometrical parameters.

Parameter			**Rissa Stage 2**	**Finneidfjord**	**Byneset**
Geometrical parameters					
Release area	A	m^2	330,000	~ 50,000	35,000
Release volume	V	m^3	$5 \cdot 10^6$	$0.2 \cdot 10^6$	$0.3 \cdot 10^6$
Gate width	W_0	m	150	100	30–50
Max. release width	W_{max}	m	500	300	125
Avg. release width	W_{avg}	m	400	250	100
Retrogression length	R	m	1400	50 (?)	400
Total run-out	L	m	2200	600	1270
Total drop height	H_t	m	56	44	42
Foreslope height	H_1	m	10	8	15
Foreslope length	L_{ct}	m	50	10	~ 40
Run-out ratio H_t/L	r	—	0.025	0.074	0.033
Foreslope angle	α	°		18	25–30
Backslope angle	β	°	2	5	1.5–5
Deposit slope angle	δ	°	0.2	3	0.9
Avg. release depth	D	m	20	2–10	8–10
Avg. deposit depth	h_D	m	6–7	2–3	3–7
Avg. deposit width	W_D	m	750	200	20–40
Geotechnical parameters					
Specific weight	γ	kN/m^3	18.6	18.8	18.3
Undrained shear strength	s_u	kPa	10–20	7–10	10–25
Remolded shear strength	$s_{u,r}$	kPa	0.24	0.08	0.12
Max. sensitivity	$S_{t,max}$	—	100	100	400
Plastic index	I_P	%	5	6	5
Liquid index	I_L	—	2.3	2.5	3.8
Destructuration index	I_D	—	0.31	0.12	0.4
Quick-clay layer depth	D_{qc}	m		0–10	3–6
Quick depth ratio D_{qc}/D	q	—		0–0.9	0.5–0.7

3 Numerical Models

3.1 BING

BING is a quasi-two-dimensional numerical model of the downslope spreading of a finite-source subaqueous debris flow (Imran et al., 2001) that incorporates the Bingham, Herschel–Bulkley (H-B), and bilinear rheologies for viscoplastic fluids. The latter was, however, not used in this study. Instead of Eqn. (1) with the consistency *K*, BING uses an equivalent formulation in terms of a reference shear rate $\dot{\gamma}_r$, at which the visco-plastic contribution to the shear stress is equal to the yield strength:

$$\frac{\dot{\gamma}}{\dot{\gamma}_r} = \begin{cases} 0 & \text{for} \quad |\tau| \leq \tau_y, \\ \operatorname{sgn}(\tau)\left(\dfrac{|\tau|}{\tau_y} - 1\right)^{1/n} & \text{for} \quad |\tau| > \tau_y. \end{cases} \tag{2}$$

As mentioned earlier, the material can deform only if the applied stress exceeds the yield strength. The Bingham rheology is a limiting case of H-B rheology with a linear stress-strain relationship for shear stresses above the yield strength, i.e., $n = 1$.

A characteristic feature of the flowing Herschel–Bulkley fluids is a region of *plug flow*, where the there is no shear because the shear stress is below the yield strength. In a free-surface gravity mass flow with negligible shear stress at the upper boundary, the plug layer extends from the upper surface some depth into the flow; underneath it is the shear layer. This is schematically indicated in Figure 12. Note that the plug layer depth generally diminishes with increasing slope angle, but it is also determined by inertial forces due to acceleration or deceleration of the flow and therefore needs to be determined dynamically.

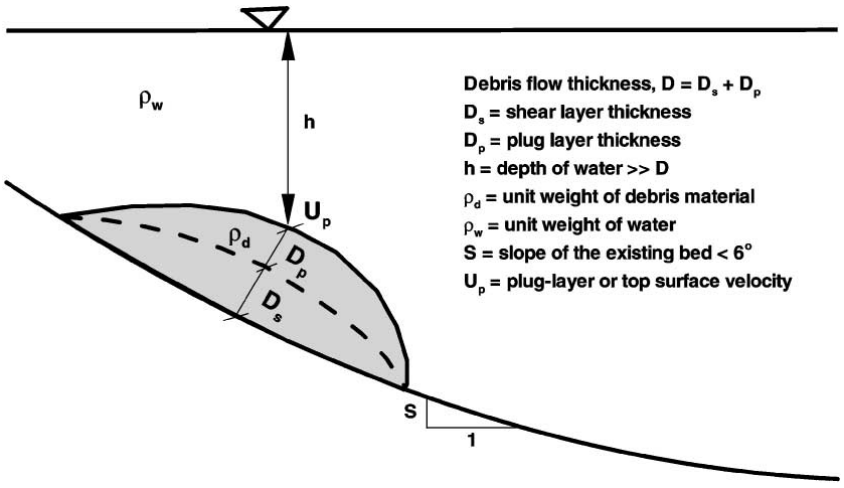

Figure 12. Definition sketch of (underwater) mudflow.

BING obtains the extra information required for determining the plug-layer depth by solving not one, but two momentum balance equations – one integrated over the entire flow depth and one integrated only over the plug layer. The formulas are not reproduced here as they are well explained in (Imran et al., 2001). As is necessary for physical consistency and closure of the equation system, the momentum balance equations are supplemented with the mass balance equation. These equations are formulated in the Lagrangian framework, i.e., in a coordinate system that moves and deforms together with the flow

The Lagrangian equations can be solved using a deformable grid system that moves together with the mass. The mass distribution is discretized into a fixed number of cells, each of which is delimited by two nodes (Figure 13). X_j denotes the location of node j and U_j denotes its velocity. The volume of each individual cell j (located between nodes j and j+1) must remain constant due to mass conservation. Thus, if the nodes defining the cell move at different velocities, the flow height in the cell changes accordingly to accommodate the stretching or squeezing. In this way, the three *partial* differential equations for $D(x,t)$, $U_p(x,t)$ and $U(x,t)$ reduce to a set of coupled *ordinary* differential equations for $X_j(t)$, $U_{p,i}(t)$ and $D_i(t)$.

By discretizing the time evolution into small time steps of duration Δt, the ordinary differential equations become difference equations, i.e., algebraic equations that can be straightforwardly solved by time-marching.

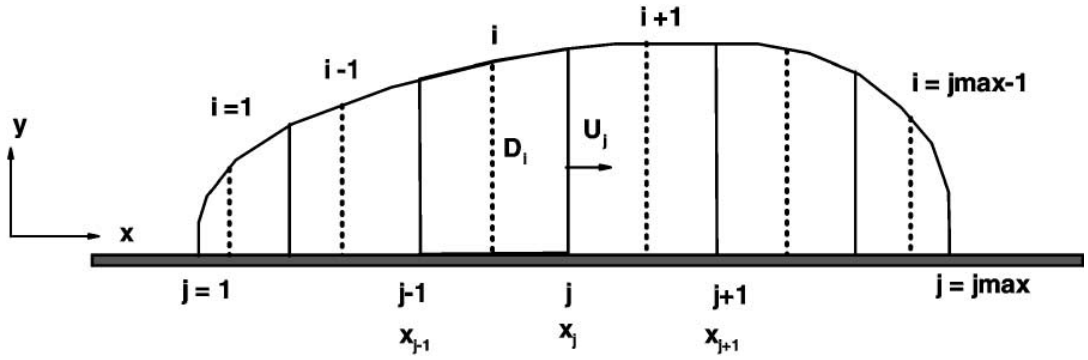

Figure 13. Discretization of the landslide mass in the Lagrangian framework: The nodes x_1, …, x_{jmax} move at velocities U_j and delimit cells of constant volume and mass, but variable length $L_j = x_{j+1} - x_j$ and height D_j.

Information to be provided to the program includes the longitudinal profile of the bed, the initial length and the initial maximum thickness of the released mass. In its original version used here, BING assumes that the initial longitudinal thickness profile of the failed material is parabolic. The material parameters describe the physical properties of the flowing slurry. In the following, the Herschel-Bulkley rheology model with an exponent n = 0.2–0.5, reflecting the shear-thinning property of clay, will be used. The values of τ_y and K (more precisely, the reference shear rate related to K by $\dot{\gamma}_r = \left(\tau_y/K\right)^{1/n}$) were adjusted to reproduce the ob-

served run-out distances. Where possible, preference was given to values of τ_y between 0.1 and 0.3 kPa, following the suggestions in (Locat and Demers, 1988).

BING takes into account buoyancy effects, which makes it also particularly suited for simulating subaqueous landslides. There is, however, no provision made for a transition from land to water, nor is it possible to start a simulation with an initial velocity. As will be seen in Sec. 0, this limitation makes it difficult to simulate the Rissa landslide from start to end. Moreover, the model does not take into account drag forces, which are important in subaqueous flows. Indeed, it has been noticed long ago that BING drastically overestimates the velocity of very large slides on long, gentle slopes (De Blasio et al., 2003).

3.2 DAN3D

This model, introduced by McDougall and Hungr (2004) and extended and described more exhaustively by McDougall (2006), utilizes the same concepts as the earlier quasi-2D model DAN (Hungr, 1995). However, the transition from describing the motion along a 1D profile line embedded in a 2D vertical plane to a 2D surface embedded in 3D space required a new approach to solving the equations: The original Lagrangian approach in DAN was similar to the one adapted by BING (see Sec. 3.1). If it is straightforwardly extended to 2D, the moving cells may deform so much that serious errors occur. One possible solution to this problem is remeshing of distorted cells, but this introduces interpolation errors that may accumulate over time and is computationally expensive. Another option is to use the Eulerian instead of the Lagrangian framework, where the computational grid is fixed in space and the material flows through the cells. Many models use this approach, but the advection terms have to be treated very carefully and the computational cost is much higher unless because the computation extends over the entire area that was or may later be reached by the landslide.

For these reasons, a *meshless* Lagrangian scheme was selected, namely Smoothed Particle Hydrodynamics (SPH, for a review see (Monaghan, 1992)): “Particles” endowed with properties corresponding to the dynamical variables move according to the equations of motion, similar to cells in conventional Lagrangian schemes. However, the field values (flow height and momentum) at a given point are not determined by the cell in which this point presently is located, but calculated as a sum of contributions from all nearby “particles”, weighted by a function of the distance between the particles and the point in question (Figure 14). The weight function or “kernel” plays a central role in the mathematical formulation of this scheme; both its shape and spatial range can be chosen freely within certain limits.

The SPH method has been successfully applied to problems that are difficult to handle with mesh techniques, e.g., the breaking of waves, the impact of droplets onto a fluid or a solid wall and other situations where the flowing material splits. If the flow dilutes very strongly in certain regions, it may be necessary to redistribute the quantities of mass and momentum carried by a single isolated “particle” over several particles newly seeded around the original one.

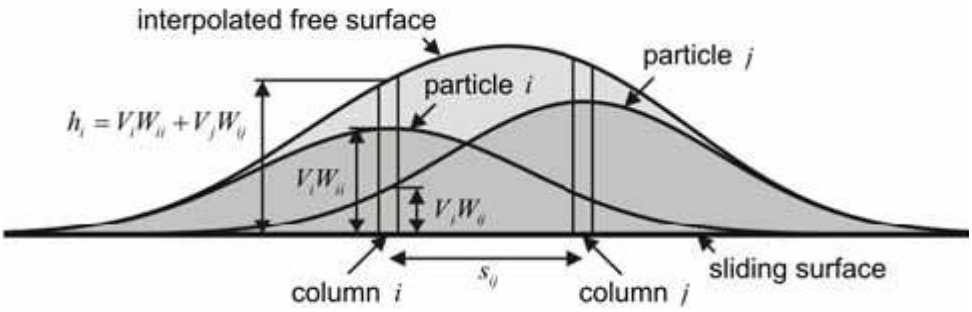

Figure 14. Schematic representation of the way SPH reconstructs the flow height (lightly shaded curve) from the weighted contributions of all particles within a finite distance (two particles i, j in this case, indicated in dark grey). V is the flow height (or mass) associated with the particles, $W(|\boldsymbol{x}-\boldsymbol{x}_i|)$ is the weight of particle i at $\boldsymbol{x}_i$ at the point $\boldsymbol{x}$. Other quantities like velocity are reconstructed in an analogous way. Figure taken from (McDougall and Hungr, 2004).

In DAN3D, the user can choose amongst five rheology types – frictional, plastic, Newtonian, Bingham, and Voellmy. The expressions for the bed shear stress are the following:

Frictional:	$\tau = (1 - r_u)\, \sigma_n \tan \varphi$	(3)
Voellmy:	$\tau = \sigma_n \tan \varphi + \gamma v^2/\xi$	(4)
Newtonian:	$\tau = 2\mu v/h$	(5)
Bingham	$\tau = \tau_y + 2\mu v/h$	(6)
Plastic:	$\tau = \tau_y$	(7)

τ is the bed shear stress, σ_n is the bed-normal total stress, φ is the apparent friction angle, γ is the unit weight of the flowing mass, v is the depth-averaged flow velocity, ξ is the turbulent friction coefficient (units m/s^2), r_u is the pore pressure ratio and φ is the dynamic basal friction angle. The plastic and the Newtonian model are limiting cases of the Bingham model with $\mu = 0$ and $\tau_y = 0$, respectively.

In contrast to BING, DAN3D is capable of taking into account entrainment of eroded bed material into the flow (McDougall and Hungr, 2005). This is an important process in debris flows and snow avalanches, but appears to play a less prominent role in quick-clay slides. The simulations with DAN3D reported in Sec. 4.2 do not make use of the entrainment routines.

The topography and the initial conditions are input in the form of three ASCII grid files in Surfer™ format (*.GRD):

- Path surface DTM: a grid file describing the ground surface of the area.
- Source thickness file: representing the difference in elevation of the ground surface before and after the slide.

- Erosion thickness file: defining the distribution of materials throughout the computation area (associated to a material number as defined in the material properties screen).

The output from DAN3D is again a set of ASCII grid files in Surfer format for the flow height and velocity at predetermined instants of time. In addition, the "particle" positions and velocities at given times can also be output.

3.3 MassMov2D

The basis for the MassMov2D model (Beguería et al., 2009) is the numerical integration of the depth-averaged equations of mass and momentum using a shallow water approximation. The implementation is performed using a finite difference scheme coded in the GIS scripting language PCRaster. The landslide mass is treated as a single phase material, which can be modelled using a Bingham or a Voellmy rheology. The original code of the model is accessible to the user for modifications. A summary of the model is presented by Quan Luna (2012).

4 Simulation results

4.1 BING

Information to be provided to BING includes the initial length and the initial maximum thickness of the slide mass, which can be taken from the literature. The numerical model parameters comprise the number of nodes and the temporal discretization, the run duration and the artificial viscosity (needed to stabilize the numerical solution). The number of nodes in the domain determines the initial grid spacing. In this study, the Bingham rheology was used in the simulations of both slides. Additionally, the Herschel-Bulkley rheology with an exponent n = 0.5, reflecting the shear-thinning property of clay, was tested in the case of the Rissa slide. The mud density was set to 1897 kg/m^3 for the Rissa landslide. The values of τ_y and μ_{HB} were adjusted to reproduce the observed run-out distance. Following (Locat and Demers, 1988), τ_y was constrained to values between 0.1 and 0.3 kPa.

In the simulations with BING, the bed profile elevation was created in a GIS by combining the pre-slide and post-slide digital elevation models. This profile was then exported to a spreadsheet containing the coordinates of the profile points, and the projected and oblique distances. Afterwards, a text file (.txt) with the downslope distance S and the elevation above an arbitrary datum was created as input to BING.

4.1.1 Byneset

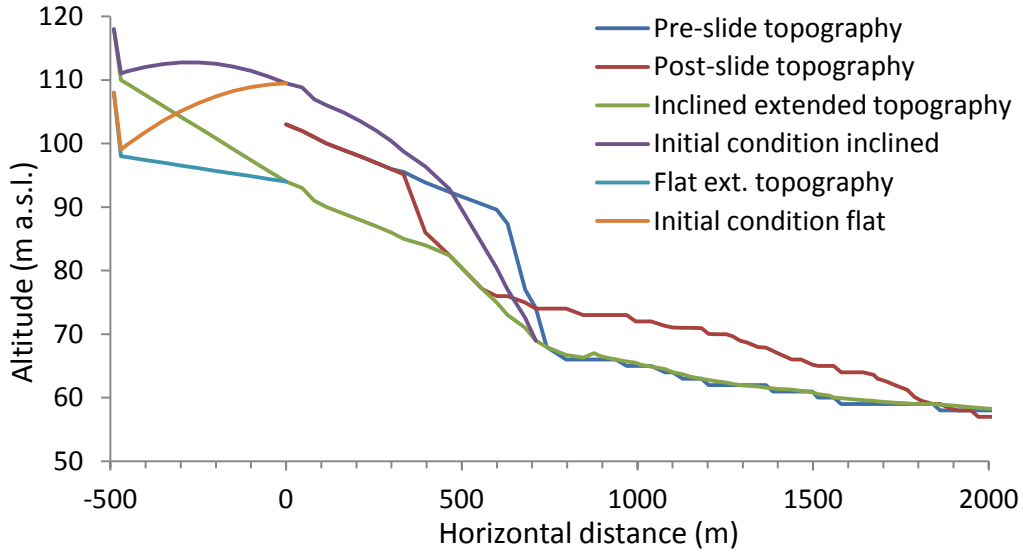

Figure 15. Pre- and post-slide topography of the Byneset slide and assumed initial conditions for the simulations with BING. See text for explanation.

In the pre-slide and post-slide digital terrain models provided by SVV, a profile line was chosen approximately in the middle of the slide crater and then along the

brook. The profile of the glide plane – obtained from the post-slide DTM inside the crater and from the pre-slide DTM further downstream – was slightly smoothed along the brook and lowered somewhat in the gate area to remove the proximal end of the deposit. In this event, the gate width is similar to the average width in the deposit area, but only about one third of the width of the release area. In order to achieve a proper representation of the deposit, the release must comprise the entire slide mass. This can be achieved by making the release area about 1200 m long instead of 400 m. Two variants for the backward extension were tested – one where the profile is continued backward with the slope of the glide plane in the crater, and another with an almost horizontal crater bottom. For comparison, runs with the actual length of the release area were also analyzed (Figure 15 and Figure 16).

The following procedure was followed: For four different values of the reference strain rate $\dot{\gamma}_r$ (5, 10, 100, 500 s^{-1}), the yield strength τ_y was varied in search of a value that reproduced the observed run-out distance within about 10 m. (Note that for a fixed reference shear rate, the consistency K is proportional to the value of τ_y). The output from all simulations was scanned for the maximum value of the front velocity. Most simulations were carried out assuming Herschel–Bulkley rheology with exponent n = 0.5 (equivalent to a Casson fluid), but for the flat extension, a corresponding series of runs with Bingham rheology (n = 1) were also recorded.

The dependence of run-out distance and maximum front velocity on the yield strength for different fixed values of the reference shear rate is shown in Figure 16–Figure 18. The main results can be summarized as follows:

- Depending on the way of accounting for the geometry of the release area, widely different values of the rheological parameters have to be used. This is connected to the flow depth, which is two to three times larger for flows with extended release area than for flows with the actual release area length.
- In all cases, the yield strength has to be chosen at least a factor of 6 larger than the undrained remolded shear strength from laboratory tests of Byneset quick clay samples.
- Pairs of values of yield strength and reference shear rate that give the same run-out distance predict similar maximum front velocities (within 10–15% for reference shear rates between 5 and 500 s^{-1}).
- For equal values of the yield strength and the reference shear rate, landslides with Bingham rheology ran typically 100–150 m longer than those with Casson rheology, even though the maximum front velocity tends to be slightly lower. This is thought to be due to the bed shear rate being less than the reference shear rate.
- The Lagrangian numerical scheme of BING exhibits erratic behavior due to the tendency for instability near the tail of the flow. Increasing the artificial viscosity can often suppress the problem, but the run-out distance and front velocity are affected by it to some degree.

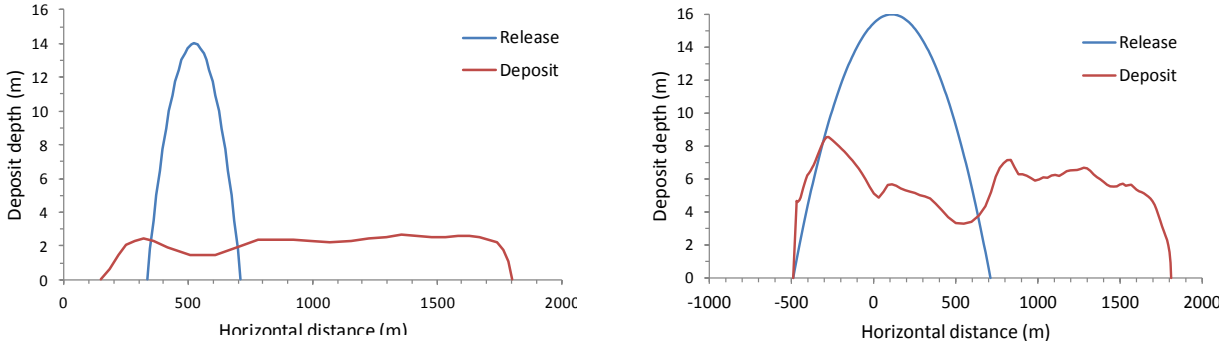

Figure 16. Release and deposit shapes for simulations of the Byneset slide with BING for original length of release area (top) and extended release area with correct starting volume (bottom).

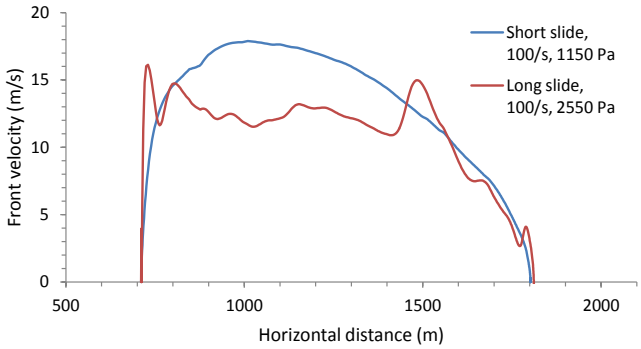

Figure 17. Evolution of front velocity along the Byneset path for short and long release areas.

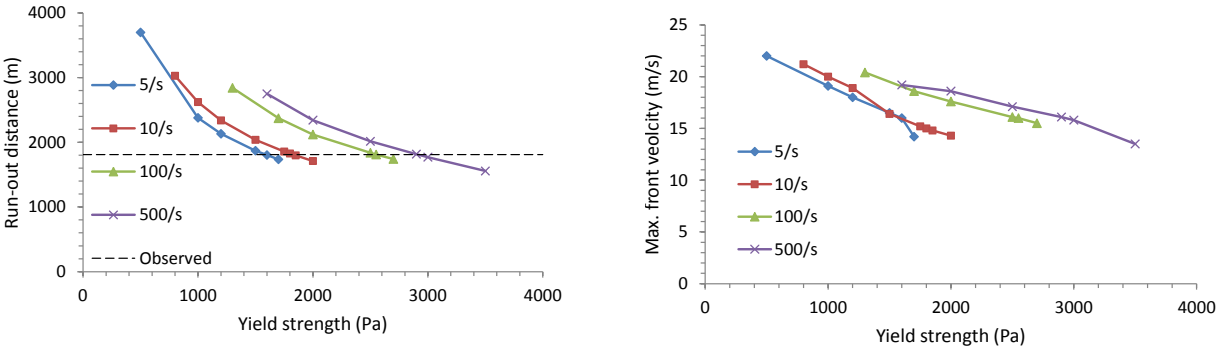

Figure 18. Dependence of the run-out distance (left panel) and maximum front velocity (right panel) on the yield strength for different values of the reference shear rate. Derived from simulations with extended flat release area.

4.1.2 Finneidfjord

The first stage of the Finneidfjord slide was purely subaqueous and can therefore be simulated by setting the density of the ambient fluid to 1020 kg/m^3. A potential problem is that the slide release area and deposit area are much wider (by a factor of 3) than the gate, giving the entire path the form of a bow-tie. BING is not designed for handling constriction and subsequent lateral expansion. However, it is not a priori clear that this makes the results invalid: Most likely, Stage 1 proceeded retrogressively so that the chunks that released simultaneously presumably comprised only a small fraction of the width of the total release area. If this is true, the port did not present a constriction. Similarly, each partial release within Stage 1 likely did not spread over the whole width of the deposit fan so that simulating the flow along a line may be adequate in this case.

However, retrogressive release also implies that it will nearly impossible to simulate the deposit profile properly with BING because the code does not accommodate multiple releases distributed over time. A (rather questionable) ad hoc procedure would be start with a partial release, modify the bathymetry for both the released and deposited mass, start a new simulation with a partial release on the modified bathymetry, etc. until the release area is exhausted. There is, however, so much arbitrariness in the choice of the partial releases that such a simulation was not attempted here.

Table 2 contains results for the first stage of the Finneidfjord landslide treated as a Bingham fluid (n = 1). The initial length and maximum thickness of the slide were set to 150 m and 5 m, respectively. As in the simulations of the Byneset slide, the observed run-out distance can be reproduced by many combinations of τ_y and μ_B, but none of them can be directly related to published geotechnical data. According to (L'Heureux et al., 2012b), the layer that failed in stage 1 consists of non-sensitive clay and silt ($S_t \approx 3$), with a water content around 35%. The undrained, unremolded shear strength is between 5 and 10 kPa. As Table 2 shows, the observed run-out distance cannot be attained with a remolded shear strength of 1.5–4 kPa, even if the Bingham viscosity is set as low as 1 mPa s. Note that BING does not take into account hydrodynamic drag, which is expected to contribute of the order of 0.1–0.5 kPa to the retarding shear stress in the present situation.

It has to be kept in mind, however, that stage 1 of the 1996 Finneidfjord slide was not a quick-clay slide. The slide material is presumably competent enough to hydroplane, there may have been lubrication due to extremely soft sediments in the flatter distal areas, etc. It should be interesting to understand the slide mechanics of the first stage more thoroughly, but this question cannot be pursued here.

For the simulations of stage 2, where a large fraction of the involved sediments were quick clay, the bathymetry was manually adjusted to reflect the glide plane. The simulations were run as subaqueous; therefore, the elevations on land were multiplied by a factor of 2.19 to offset the buoyancy effect. Both Bingham and Casson rheologies were tested. See Table 3 for parameter combinations that reproduced the observed run-out distance reasonably well.

Table 2. Input parameters and output from BING simulation for Stage 1 of the Finneidfjord landslide with Bingham rheology (exponent n = 1). The initial length and the maximum initial thickness of the slide are 150 m and 5 m, respectively, for all simulations. The run-out distance is measured from the shoreline.

INPUT				*OUTPUT*	
Yield Strength (Pa)	*Reference shear rate (1/s)*	*Ambient fluid density (kg/m³)*	*Mud density (kg/m³)*	*Run-out distance (m)*	*Max. front velocity (m/s)*
50	0.63			771	15.4
100	1.27			629	14.8
150	1.91			566	15.6
200	2.55			531	15.1
250	3.18			496	15.2
300	3.82			472	15.6
350	4.45			454	15.1
400	5.10			441	14.4
450	5.73			430	15.5
500	6.36			422	15.9
300	10			547	14.3
300	20	1020	1880	605	14.8
300	50			674	14.7
300	100			775	18.2
300	200			840	18.8
300	500			913	19.0
500	10.0			449	14.5
500	20			493	14.4
500	50			551	14.4
500	100			607	16.9
500	200			643	17.4
500	500			684	17.7
1000	10^6			480	17.7

It is evident from Table 3 that the observed run-out distance cannot be reproduced with parameter values that are typical of quick clays. For example, if a Bingham fluid with yield strength 350 Pa is assumed, the viscosity has to be chosen as 350 Pa s—a value that is more than three orders of magnitude higher than what is expected. If one chooses a suitably low viscosity, the yield strength must be of the order of 2 kPa or a factor of 5 above the conventional limit for quick clays. Similar conclusions apply to the Casson rheology.

Table 3. Summary of simulations of stage 2 of the Finneidfjord slide with BING. Only the runs that best matched the observed run-out distance are shown for the Bingham rheology. The ambient fluid density and the sediment density are set to 1020 and 1880 kg/m^3, respectively.

INPUT			*OUTPUT*	
Exponent n (—)	*Yield strength (Pa)*	*Consistency (Pa s$^{n)}$*	*Run-out distance (m)*	*Max. front velocity (m/s)*
1.0	350	350	905	14.4
	1000	100	899	16.2
	1300	65	877	16.1
	1500	30	896	15.9
	1600	16	911	16.1
	1800	9	887	17.4
	1850	4	912	16.0
0.5	500	22	1811	20.9
		29	1748	20.8
		50	1597	20.5
		158	1238	17.8
		500	887	16.2
	750	75	1270	19.7
	1000	100	1082	19.0
	1250	125	955	18.4
	1350	135	913	18.2
	1500	150	910	16.1

4.1.3 Rissa

The major challenges in simulating the Rissa slide stage 2 with BING are the following:

1. Stage 2 consisted of several flake releases, the first two of which were the largest and best documented, followed by more continuous retrogressive release of smaller quantities of soil. Complete simulation of the entire Stage 2 does not appear feasible with BING; one has to choose either one of the flakes or the subsequent retrogressive failure.
2. The first flake had to open the gate and therefore did not reach as high velocity as the subsequent flake did. Simulating the run-out of the first flake in a realistic way appears to be outside BING's capacity.
3. It is neither possible to specify different ambient-fluid densities for the subaerial and the subaqueous parts of the path, nor to run a subaerial simulation to the lakeshore and to use the final state as starting condition for a subaqueous simulation from lakeshore to run-out.

4. If the correct value of the yield strength is chosen for the basal quick-clay layer, BING will simulate shearing also in parts of the non-sensitive soil on top and thus predict too high velocity (also leading to longer run-out). This is a consequence of assuming a single material with constant properties.

A first round of simulations attempted to mimic the situation in future applications of a run-out model, with only the areal extent of the quick-clay zone known. The entire stage 2 slide was treated as a single release with a length of 500 m and a maximum depth of 20 m (corresponding to an average depth 13.3 m as BING assumes a parabolically shaped release mass). Both the Bingham (n = 1) and the Casson (n = 0.5) rheologies were tested. The simulations were run once as completely subaerial and once as completely subaqueous. The yield strength was varied in the typical range of quick clay between 0.05 and 0.35 kPa. For the Bingham fluid, the (Bingham) viscosity was estimated from the liquidity index I_L using a correlation proposed by Locat and Demers (1988) on the basis of extensive laboratory tests of Canadian quick clays:

$$\eta = \left(\frac{9.27}{I_L}\right)^{3.33} \text{ mPa s.} \tag{8}$$

As noted by L'Heureux (2012b), Norwegian quick clays differ from Canadian ones and this relation may not hold for the Rissa quick clay, but for lack of corresponding measurements on Norwegian clays, (8) was nevertheless used. No similar relations have been proposed for Herschel–Bulkley or Casson rheology. For simplicity, the same reference shear rates were also used in the non-Bingham case. The results are tabulated in Table 4 for a Bingham fluid and in Table 5 for a Casson fluid. Note, however, that it was discovered during the write-up of this report that a factor of 10^3 was left out in the conversion from viscosity to reference shear rates. See below for the conclusions that can nevertheless be drawn from those simulations.

L'Heureux et al. (2012a) did not attempt to simulate the first flake, but concentrated on the second to circumvent the problem of blocking and squeezing, which lies outside the capacity of BING. The same will be done here in a second round of simulations. In order to deal with the third problem, the following approach is adopted: Buoyancy reduces the gravitational force in water by a factor $1 - \rho_w/\rho_{qc} \approx 0.46$, but the inertial forces remain the same and (for visco-plastic rheology in contrast to frictional) also the bed resistance. This effect can be mimicked accurately by reducing the bathymetry by a factor of 0.46. It is not possible, however, to account for hydrodynamic drag in the original version of BING. The fourth issue cannot be addressed with BING other than by choosing a somewhat higher yield strength and consistency than the quick clay has so as to compensate for the excessively thick shear layer.

Table 4. Input parameters and output from BING simulation for Rissa landslide with Bingham fluid. The release length was set at 500 m and the maximum release thickness at 20 m. The front location is measured the rearmost point of the crown.

INPUT				*OUTPUT*	
Yield strength (Pa)	*Reference shear rate (1/s)*	*Ambient fluid density (kg/m³)*	*Mud density (kg/m³)*	*Front location (m)*	*Max_front velocity (m/s)*
100	0.96	1000	1897	4821	18.0
150	1.45	1000	1897	4295	16.7
200	1.93	1000	1897	3971	15.5
250	2.41	1000	1897	3689	14.4
300	2.89	1000	1897	3408	13.7
350	3.37	1000	1897	3098	13.3
100	0.96	1	1897	6486	29.8
150	1.45	1	1897	5749	27.6
200	1.93	1	1897	5255	27.1
250	2.41	1	1897	4900	26.3
300	2.89	1	1897	4633	25.5
350	3.37	1	1897	4419	24.8

Table 5. Input parameters and output from BING simulation for Rissa landslide with Herschel-Bulkley exponent n = 0.5 (shear-thinning fluid). The release length was set at 500 m and the maximum release thickness at 20 m. The front location is measured the rearmost point of the slide scar.

INPUT				*OUTPUT*	
Yield strength (Pa)	*Reference shear rate (1/s)*	*Ambient fluid density (kg/m³)*	*Mud density (kg/m³)*	*Front location (m)*	*Max_front velocity (m/s)*
50	0.23	1000	1897	5091	18.4
100	0.96	1000	1897	4787	17.9
150	1.45	1000	1897	4528	17.4
200	1.93	1000	1897	4311	16.9
250	2.41	1000	1897	4119	16.3
300	2.89	1000	1897	3962	15.8
350	3.37	1000	1897	3803	15.3
50	0.23	1	1897	6734	30.6
100	0.96	1	1897	6430	29.6
150	1.45	1	1897	6154	28.8
200	1.93	1	1897	5911	28.3
250	2.41	1	1897	5672	27.8
300	2.89	1	1897	5452	27.3
350	3.37	1	1897	5248	27.1

Table 6. Simulations of the run-out (distance measured from lakeshore) of flake B in the 1978 Rissa slide with BING, assuming a Herschel–Bulkley fluid with n = 0.5. The simulations that most closely match the observed emplacement of the flake are marked in grey.

INPUT			*OUTPUT*		
Max. release depth (m)	*Yield strength τ_y (kPa)*	*Ref. shear rate $\dot{\gamma}_r$ (s^{-1})*	*Run-out distance (m)*	*Max. speed on land (m/s)*	*Max. speed in water (m/s)*
7	180	10	893	14.4	17.2
7	180	20	1056	14.8	18.1
7	180	25	1111	14.9	18.3
7	180	30	1157	14.9	18.5
7	180	50	1284	15.1	18.9
7	180	100	1417	15.1	19.4
10	180	5	1135	16.7	19.3
10	190	5	1095	16.7	19.2
10	200	5	1045	16.5	18.8
10	180	10	1329	17.1	20.3
10	200	10	1230	16.9	19.8
10	220	10	1142	16.7	19.4
10	230	10	1103	16.6	19.2
10	240	10	1066	16.5	19.0
10	250	10	1036	16.5	19.0
10	275	10	959	16.4	18.5
10	275	20	1114	16.7	19.4
10	300	20	1036	16.5	19.0
10	350	20	904	16.2	18.3
10	350	50	1077	16.6	19.3
10	375	50	1013	16.5	19.0
10	300	100	1375	17.1	20.4
10	350	100	1206	16.8	19.9
10	375	100	1130	16.7	19.6
10	400	100	1069	16.6	19.3
10	300	200	1513	17.3	20.8
10	400	200	1172	16.8	19.7
10	425	200	1110	16.6	19.5
10	450	200	1051	16.5	19.3
10	500	200	949	16.3	18.9
10	300	500	1673	17.4	21.2
10	400	500	1293	16.8	20.2
10	475	500	1100	16.4	19.5
10	500	500	1047	16.3	19.2

Table 6 shows the simulated runout distance and maximum front velocity of flake B for different values of the yield strength and reference shear rate. The initial length of the slide mass was kept constant at 200 m while the maximum release depth was set to 10 m for most simulations and to 7 m in some additional runs in order to quantify the effect of this parameter.

The main observations from both types of simulations are the following:

- As expected, purely subaerial simulations have much longer run-out than subaqueous ones (in this case, the difference is typically 1.5 km). In reality, hydroplaning and other effects may cause subaqueous flows to have longer run-out.
- Simulating the entire stage 2 flow as a simultaneous release with rheological parameters in the range typical of quick clays predicts run-out distances that are between 1.5 and 4 km too long.
- Simulations with $n = 0.5$ have substantially longer run-out than those with $n = 1.0$ and the same value of the reference shear rate. This indicates that the shear rate is predominantly larger than the reference shear rate. This translates into the velocity being above the threshold where the viscous contribution to the resistance exceeds the plastic one.
- Simulating flake B only and assuming a thinner flake (7–10 m), the observed run-out distance can be reproduced with rheological parameters that are reasonably close to the measured soil properties. If hydrodynamic drag were taken into account, the yield strength should be chosen lower and/or the reference shear rate higher than indicated in Table 6.
- The run-out distance grows roughly proportional with the release depth.
- Somewhat surprisingly, the maximum front velocities both on shore and off shore do not differ much for different combinations of the yield strength and consistency that give the same run-out distance. They depend on the flow depth and the flow resistance, however.
- Within the tested range of yield strengths, the simulated velocity on land is 60–70% higher than observed. Judging from tsunami simulations (L'Heureux et al., 2012), the simulated velocity in water is too high by a factor of 1.5–2.
- In all simulations of flake B, the flow front nearly comes to a stop some place between 700 and 1000 m from the lakeshore. When a strong surge from the rear reaches the front, the front velocity quickly rises and reaches values close to maximum front speed, which is attained in the steepest part of the profile about 100 m off shore. Due to this, the front travels several hundred meters longer than it would without the surge.
- Further scrutiny of the simulations is needed to understand why the peak velocity is *lower* in (subaqueous) simulations of the entire stage 2 (with a maximum release depth of 20 m and much longer run-out) than in simulations of flake B.

4.2 DAN3D

Information to be provided to DAN3D includes the digital terrain model of the landslide path and a digital elevation model of the depth in the release area. The version of DAN3D available for this project is Release 001, which was compiled on 29 January 2009. This code was kindly provided to ICG/NGI by Prof. Oldrich Hungr for use in research projects. The numerical model parameters comprise the temporal discretization, the number of particles, the run duration and other parameters needed to stabilize the numerical solution. The number of nodes in the domain is restricted to a maximum of 1000 per axis. In this study, the Bingham and the plastic rheologies were tested (see Sec. 3.2 for details)..

In the simulations with DAN3D, the path topography was created in a GIS by creating a terrain model from 1-m contours on land. Since DAN3D has been developed for subaerial landslides, the terrain model was adapted for submarine conditions (in order to account for the effect of the submerged weight in the driving forces) in the same way as for BING (see Sec. 0).

4.2.1 Byneset

The landslide was initially simulated using a Bingham model for the rheology with the following two scenarios:

a. Yield strength = 0.12 kPa and viscosity = 1.95×10^{-5} kPa·s
b. Yield strength = 0.12 kPa and viscosity = 0.19 kPa·s

The choice of yield strength is based on actual measurements of remolded strength of the slide material reported by Thakur and Degago (2012). The viscosity for scenario (a) is obtained from empirical relation Eq. (8) proposed by Locat and Demers (1988) and the liquidity index reported by Thakur and Degago (2012). The viscosity in scenario (b) was estimated by Edgers and Karlsrud (1982) using material from the Rissa quick-clay slide.

During the simulations with the Bingham rheology, the movement of the landslide stopped after the first time step. It should be noted that DAN3D has been benchmarked and tested successfully using the frictional and Voellmy rheologies, but as far as the authors are aware, there are no reports in the literature regarding the use of this model with cohesive rheologies (Bingham and plastic).

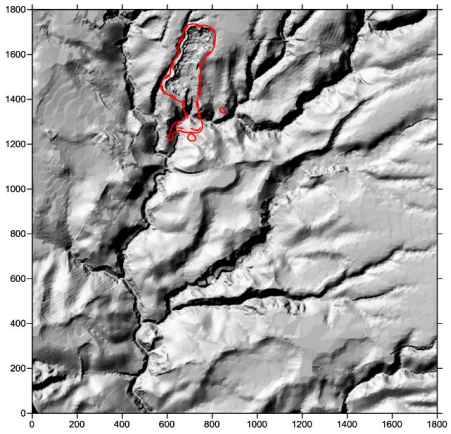

(A) t = 20 s

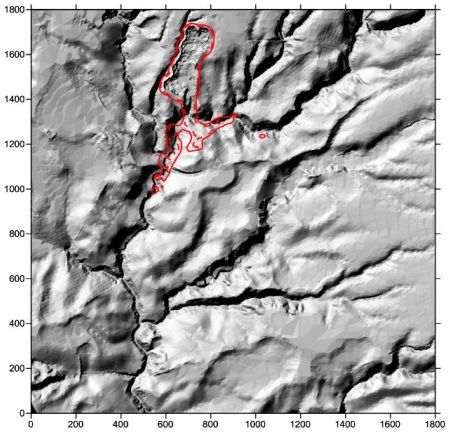

(B) t = 40 s

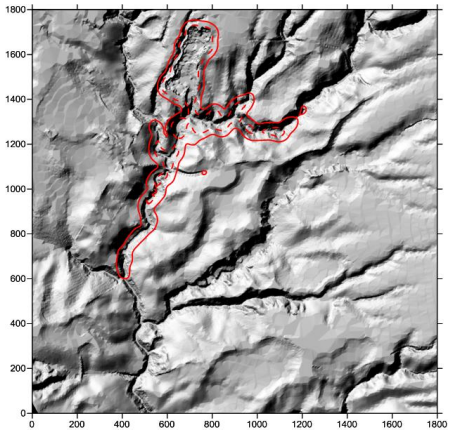

(C) t = 100 s

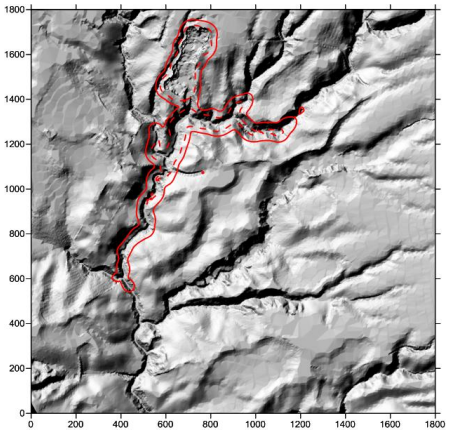

(D) t = 200 s

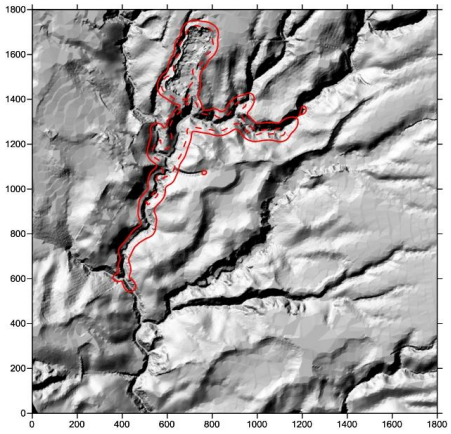

(E) t = 400 s

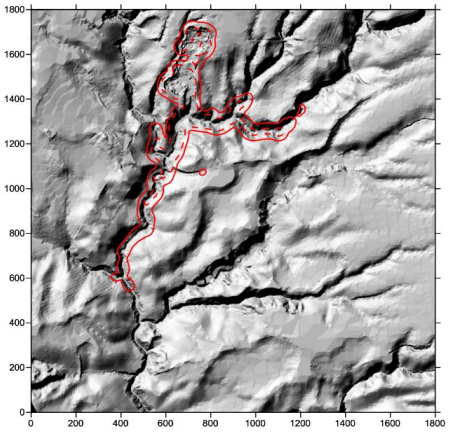

(F) t = 800 s

Figure 19. Simulation of the 2012 Byneset slide with DAN3D: Contours of flow/deposit depth. Full and dashed lines lines correspond to deposit depths of 0.1 m and 1.0 m, respectively. Plastic rheology with yield strength set to 0.12 kPa.

An additional simulation was performed by assuming a plastic model (i.e., zero viscosity) with the aforementioned value of yield strength (0.12 kPa). The results of this simulation are shown in Figure 19. The footprint of the final deposit (Figure 19.f) agrees quite well with the actual deposit shown in Figure 11. The spatial distribution has also a good agreement regarding the thinning deposit towards the maximum run-out and the continuous deposition starting from the outlet of the scarp. However, the order of the values of the simulated flow depth is quite low relative to the observed deposition. The actual deposit is relatively thick down to the maximum run-out extent (some 3 m at the terminal), while the simulated flow is thinning from 1 m to 0.1 m during the last 200 m of run-out along the main channel.

The fact that the model did not have an early stop with a plastic model, as opposed to the Bingham model with the same yield strength (i.e., a more rigid rheology), indicates that the version of DAN3D that was tested in this project seems to need further development for these cohesive rheologies (at least for the Bingham model).

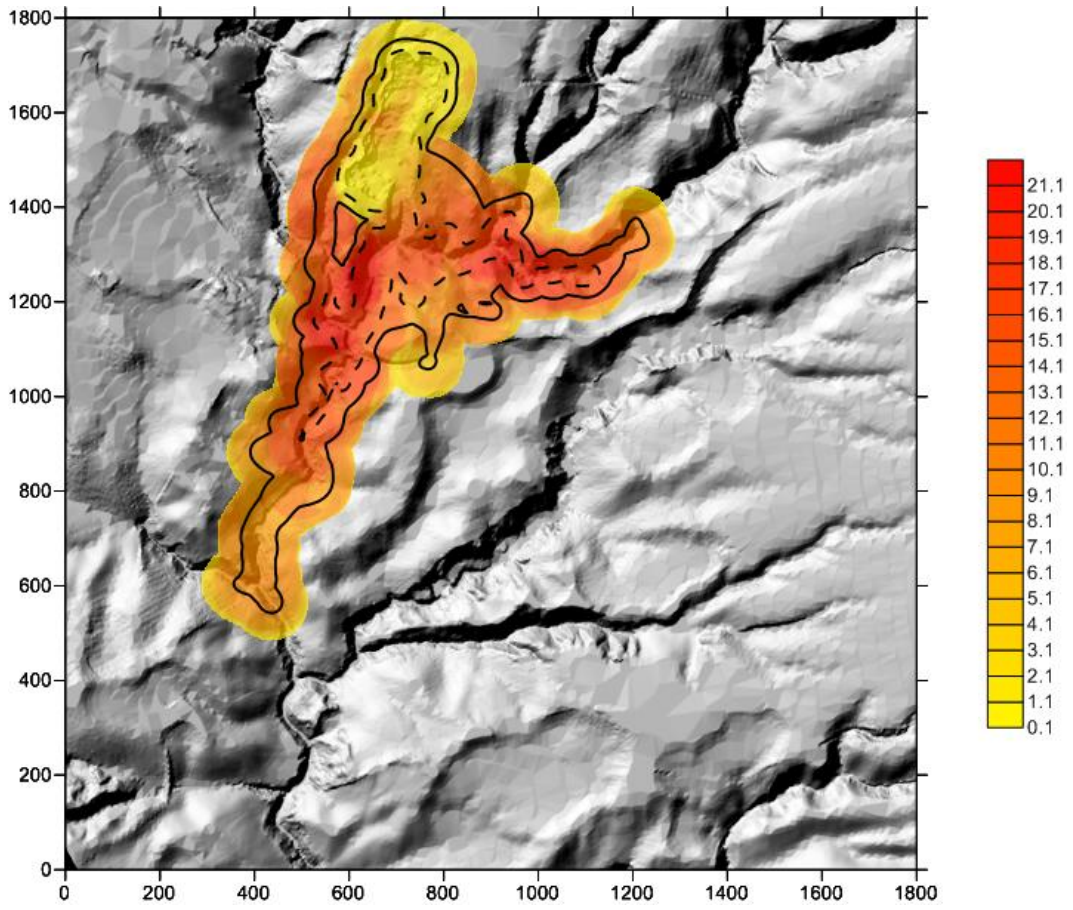

Figure 20. Simulation of the 2012 Byneset slide with DAN3D: distribution of maximum flow velocities. Labels in colour bar are in m/s. Full and dashed lines correspond to maximum simulated flow depths of 0.1 m and 1.0 m, respectively. Plastic rheology with yield strength set to 0.12 kPa.

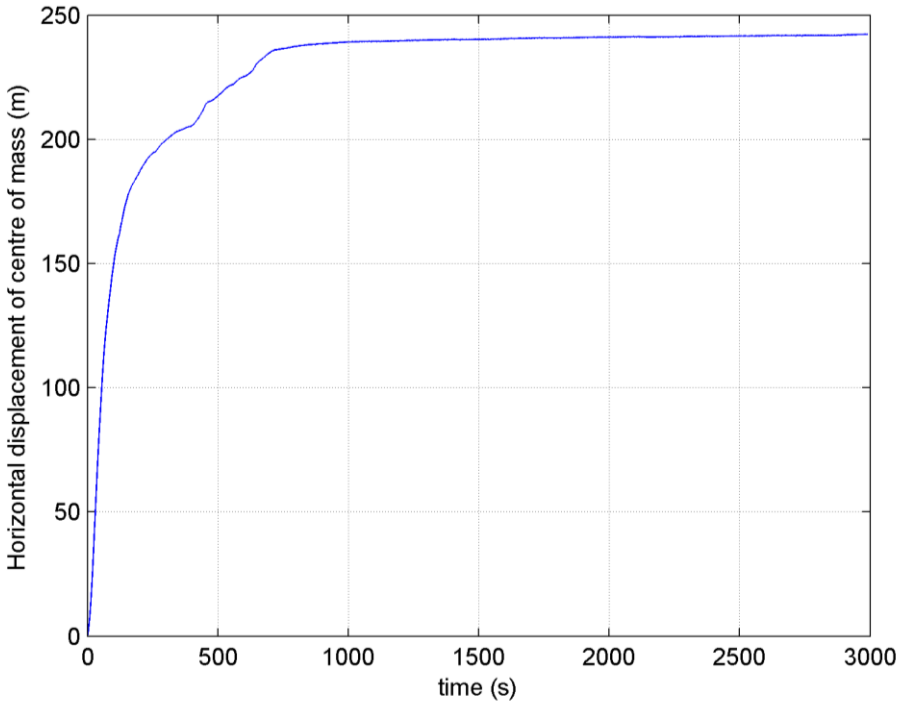

(A)

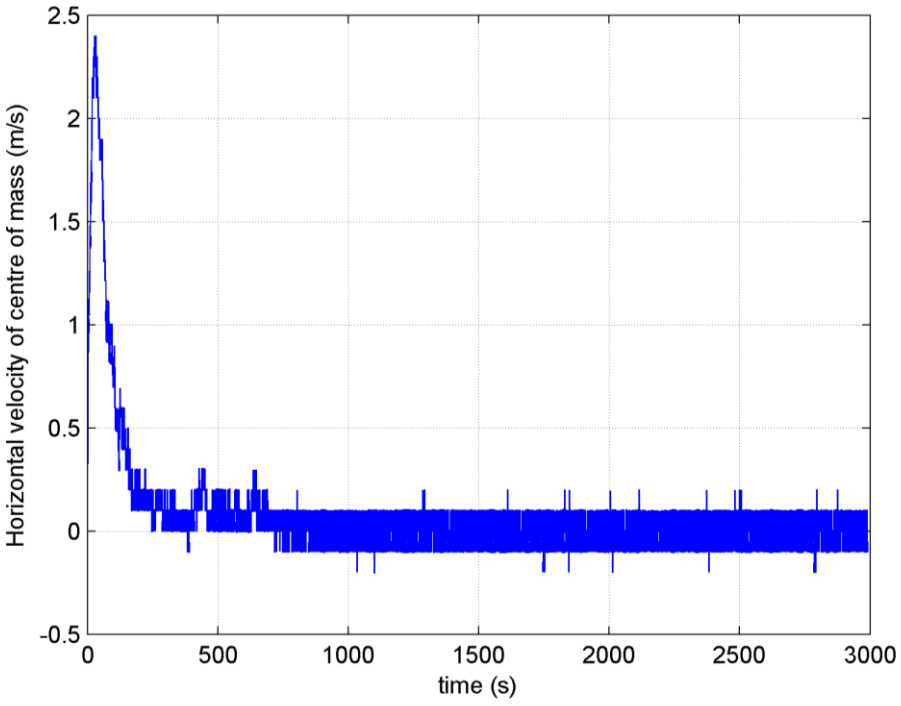

(B)

Figure 21. Time evolution of center-of-mass displacement (A) and velocity (B) for a simulation of the 2012 Byneset slide with DAN3D, using the plastic rheology with yield strength 0.12 kPa.

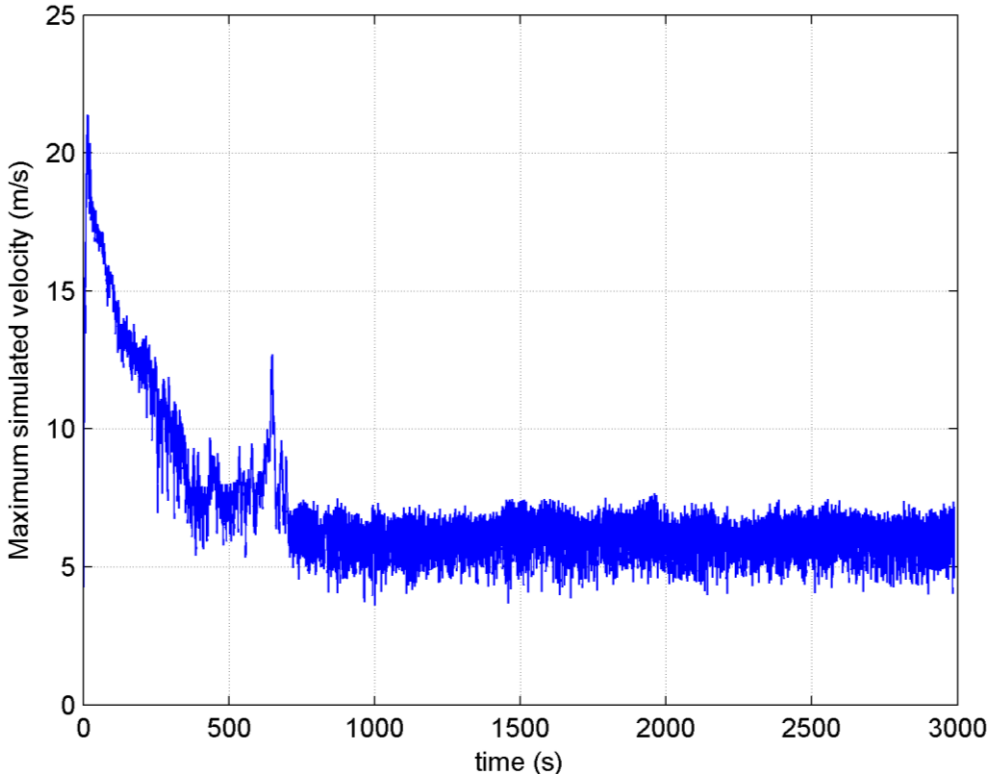

Figure 22. Time evolution of maximum velocity for a simulation of the 2012 Byneset slide with DAN3D, using the plastic rheology with yield strength 0.12 kPa.

The maximum simulated flow velocities are about 20 m/s, and occur just downstream from the gate area (see Figure 20). It is interesting to note that the maximum flow velocity within the scarp area and at the maximum run-out distance along the main north-south channel barely reaches 10 m/s.

The time evolution of the simulated displacement and velocity of the centre of mass of the landslide are presented in Figure 21. Two important aspects can be remarked: the landslide is stopping at about 800 s (actually the front is stopping much earlier, as indicated in Figure 19.d, e, and f), and there are oscillations in the landslide mass after this time. These oscillations are also reflected in the time evolution of the maximum velocity (Figure 22) and have been previously observed by Cepeda (2008) in the DAN3D simulation of a landslide in Hong Kong. These oscillations are most likely numerical artifacts, though this issue deserves further examination.

4.2.2 Finneidfjord

Since DAN3D does not account for buoyancy in the simulation of submarine landslides, the bathymetry of the submarine part of the surface was modified in order to approximate the effect of buoyancy by reducing the water depth by a factor of $1 - \rho_w/\rho_{qc} \approx 0.457$ everywhere, as was done for BING in some cases.

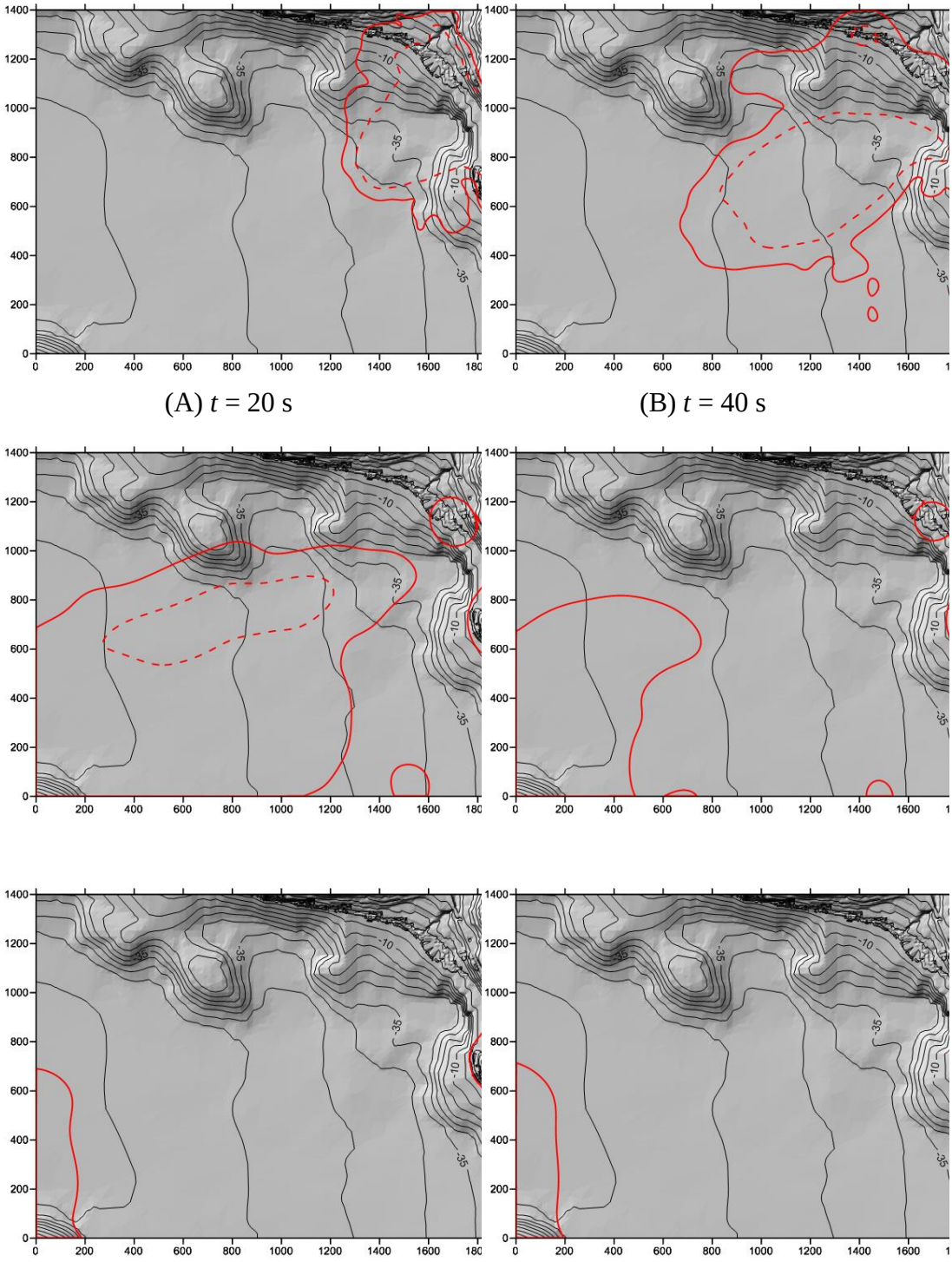

Figure 23. Simulation of the 1996 Finneidfjord slide with DAN3D: Contours of flow/deposit depth. Full and dashed lines correspond to deposit depths of 0.1 m and 1.0 m, respectively. Note that virtually no sediment is deposited where it is observed in reality. Plastic rheology with yield strength set to 0.08 kPa.

A plastic rheology with the yield strength set to 0.08 kPa (Natterøy, 2011) was employed in the simulation. The time evolution of the flow depth is presented in Figure 23. The observed deposits left along the landslide path (see Figure 8) are not reproduced in the present simulation.

The spatial distribution of maximum velocities during the flow simulation is shown in Figure 24. The maximum velocity is in the range of 30–35 m/s. Even though no velocity estimates are available for this event, it appears that the simulated values are far too high: Rapid acceleration of close to 10^6 m^3 of sediment and displacement of this mass at such velocities in the relatively shallow fjord would presumably have generated a noticeable tsunami, but no such observations are recorded. This simulation thus raises similar questions as the ones performed with BING (Sec. 4.1.2).

As in the Byneset simulations, spurious high velocities are predicted by the model in vast areas with very small flow depth. Again, this effect is largely attributable to the relatively low number of "particles" with correspondingly large domain of influence that were employed in the simulation in order to keep the computation time within practical limits.

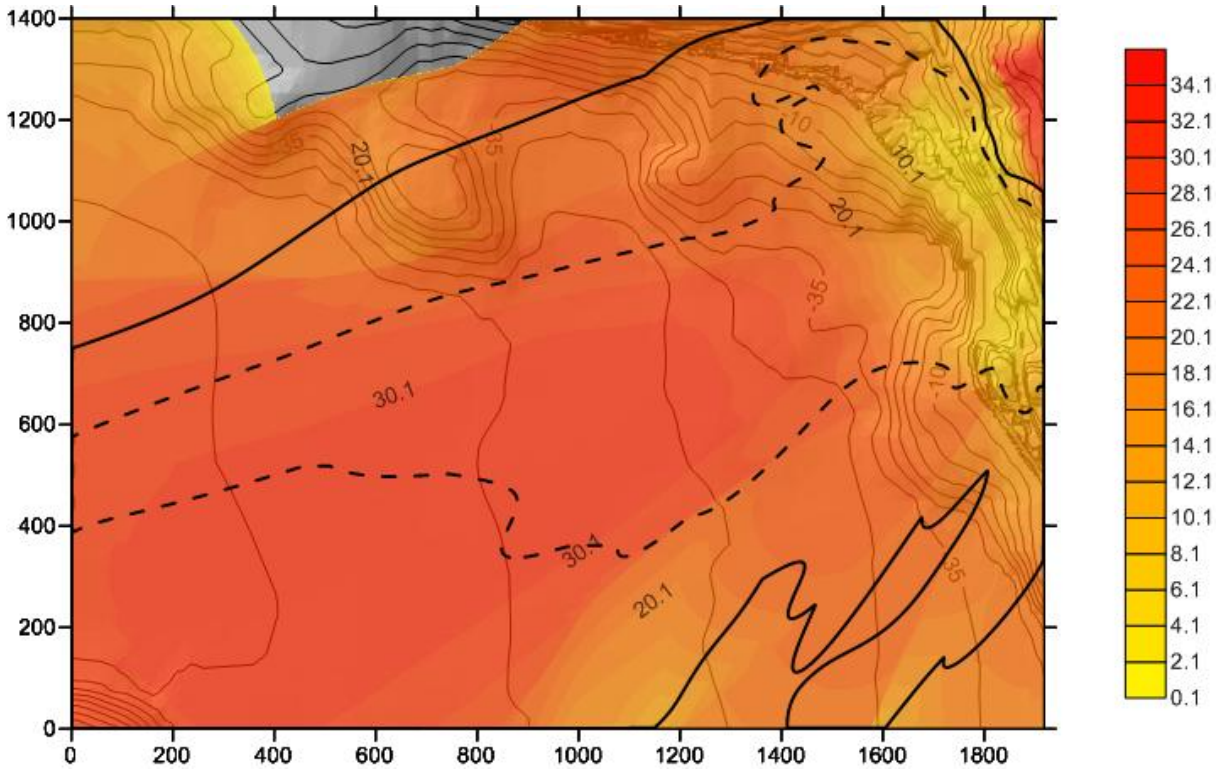

Figure 24. Simulation of the 1996 Finneidfjord slide with DAN3D: distribution of maximum flow velocities. Labels in color bar are in m/s. Full and dashed lines correspond to maximum simulated flow depths of 0.1 m and 1.0 m, respectively. Plastic rheology with yield strength set to 0.08 kPa.

4.3 MassMov2D

The simulations with the MassMov2D model had the purpose of performing a comparison with the simulations with DAN3D, using the same rheological assumption, digital terrain model and release volume, but a different numerical scheme. The use of the MassMov2D model was not originally planned for this project. Since this model became available only at the very end of this project, the results are to be considered tentative compared to the ones obtained with BING and DAN3D. Only the Byneset case was analysed with MassMov2D.

The results of the simulations with MassMov2D are shown in Figure 25. Three observations are noteworthy because they disagree with the observed deposit distribution:

- The deposit thickens towards its distal end.
- Almost no final deposition is simulated for several hundred meters downstream from the outlet of the scarp area.
- The simulated maximum run-out is substantially longer than the observed one (in fact, the simulated flow front has not completely come to rest after 800 s).

A practical advantage of MassMov2D over DAN3D is that computations are significantly faster. Moreover, despite the general tendency of Eulerian numerical schemes to be diffusive, spurious high velocities connected to unrealistically low flow depths are not observed to the same degree as in DAN3D, the flow is essentially confined to the ravine (Figure 25).

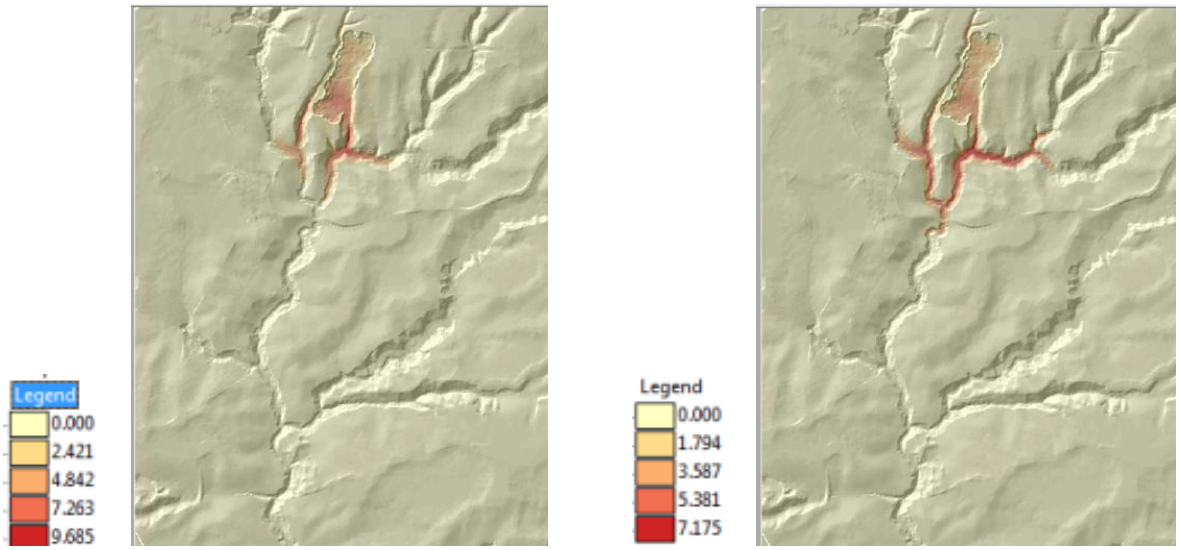

(A) t = 100 s (B) t = 200 s

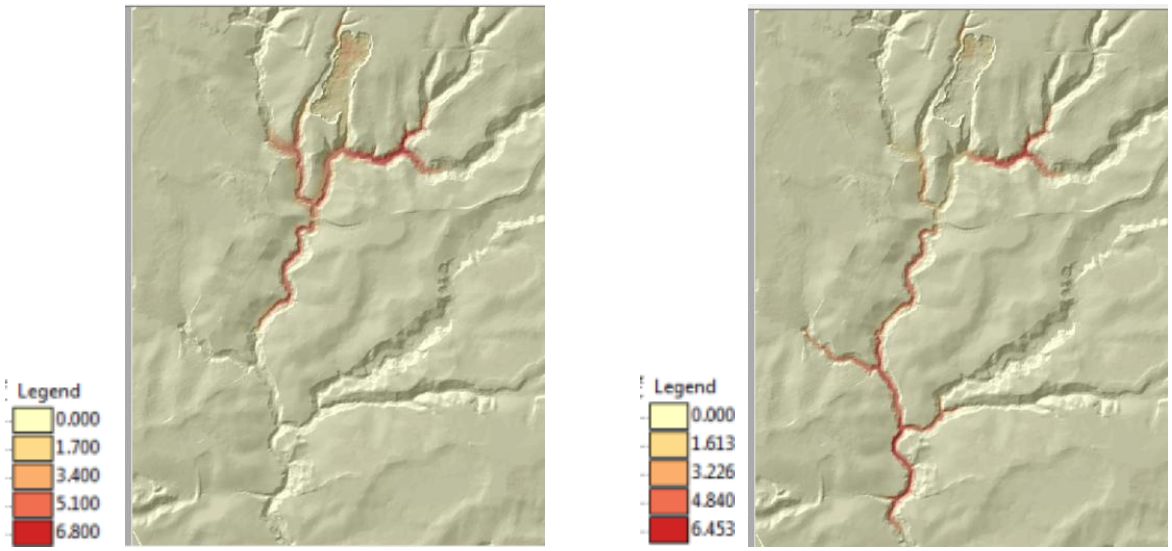

(C) t = 300 s (D) t = 400 s

Figure 25. Simulation of the 2012 Byneset slide with MassMov2D: maps show flow/deposit depth at the specified times. Plastic rheology with yield strength set to 0.12 kPa.

5 Discussion and conclusions

The following discussion will touch upon the following issues: (i) Is there enough observational material from quick-clay slides available to allow the validation (or rejection) of specific run-out models? (ii) What can be said about the qualities and shortcomings specifically of BING, DAN3D and MassMov2D? (iii) What conclusions can be drawn concerning the development of a new run-out model specifically aimed at quick-clay slides?

5.1 The need for field data in the validation of models

The quick-clay slides selected for this study are certainly among the best-documented and investigated. Nevertheless, the attempts to simulate these flows revealed several points where information is missing or not readily accessible. Therefore, assumptions regarding the initial conditions had to be made and the degree to which the model predictions could be verified was limited:

- The pre-slide topography or bathymetry is poorly known in many cases—usually, a detailed terrain model is elaborated only after the event and if there is need for detailed maps to support the planning of mitigation measures.
- The volumes and timing of retrogressive partial releases are often unknown.
- Velocity estimates are available only in exceptional cases. The velocity along the flow path is perhaps the most discriminating measurement when it comes to verifying rheological assumptions because the run-out distance can be reproduced by adjusting one suitable model parameter whereas the evolution of the velocity contains information on the internal mechanisms in the slide.
- Finally, as pointed out by L'Heureux (2012b), there is a strong need for laboratory testing of quick clays in order to better understand their rheology. The pioneering analysis by Locat and Demers (1988) assumes a Bingham fluid, even though the data seem to favor a shear-thinning visco-plastic model with a presumably rather low exponent $n < 0.5$. Given that there are non-negligible differences between Canadian and Scandinavian quick clays, similar measurements should be done on the latter as were done on the former.

5.2 Remarks concerning the performance of the tested models

BING has proved to be a model that is easy to use and delivers results quickly. Its user interface is simple and intuitive. The headers of its output files contain most of the key information on the specific run; what is missing for use in consulting projects, could easily be added in the source code. Providing options for saving plots as graphics files presumably requires some extra work. Any development on the original code is, however, hampered by the fact that VisualBasic as a pro-

gramming language is limited to MS Windows as a host and is no longer maintained and developed by Microsoft.

The numerical scheme of BING should be quite robust. Nevertheless, numerical instabilities are encountered quite frequently, most often in the tail of the flow. Tuning the amount of artificial viscosity most often allows carrying out the simulation nevertheless, but the results depend to some degree on the amount of damping. Work on a new implementation of BING and variants thereof revealed moreover that approximations made in the calculation of the shear-layer depth may cause negative shear-layer depths in the starting or stopping phase of the flow. This issue will be investigated further in the near future in another project.

DAN3D: Simulations using the Bingham rheology were attempted but the landslide came to a full stop within the first time step (0.1 s), so a plastic rheology had to be used instead. This might indicate that the version of DAN3D available for this project (compiled on 29 January 2009) has not fully implemented the Bingham rheology yet. It remains to be seen whether more recent versions have overcome this problem. A most welcome improvement of the code would be higher efficiency that would reduce the time required for a simulation of a moderately large problem like Byneset from several hours to less than an hour all the while allowing the use of many more "particles". This would presumably help a long way to control the diffusion of mass and the strong fluctuations inside the moving mass, and give better agreement between the observed and simulated deposit depths (which differed by an order of magnitude over large areas in the Byneset simulations).Another desirable feature is the possibility to start a simulation using output from a previous simulation as input.

MassMov2D: With identical terrain models, starting conditions, and rheological parameters, DAN3D and MassMov2D produced significantly different results for the Byneset landslide, both in run-out time and distances, and in the pattern of deposition. The DAN3D simulation shows closer agreement with the observed deposits, whereas the one from MassMov2D differs significantly, most remarkably in the pattern of deposition, which is reminiscent of a frictional material rather than a cohesive one (e.g., no simulated deposit in the upstream parts of the main channel). However, no definitive conclusions concerning MassMov2D can be drawn at this point.

5.3 Pointers towards future work

Quasi-2D vs. quasi-3D models: The two models that were tested on 3D terrain (DAN3D and MassMov2D) have a significant advantage over 1D models when simulating landslides with branching and run-up, such as in the case of the Byneset landslide. BING, on the other hand, is a superb tool for quickly testing ideas and scanning the parameter space thanks to its minimalistic requirements on topographic data and computer resources. It appears clear that future development work has to aim for a quasi-3D model, but there is also use for a quasi-2D model for quick-clay slides.

Dynamical or empirical models: Based on the experience gained in the course of this work, the authors think that a quasi-2D model may prove more reliable and easier to use than purely empirical models based on topography and statistical correlations only. The main reason for this is that the setting of potential quick-clay slides is so variable with respect to soil layering and soil parameters, and release area and path geometry that the available data from past quick-clay slides may not be sufficient to obtain useful correlations. However, only future dedicated work in both directions will be able to give a definite answer.

Necessary ingredients in a future dynamical quick-clay slide model:

1. *Inclusion of retrogression:* All three slides used in this study developed retrogressively at least in certain stages, but they were modeled as instantaneous releases. This can influence the computed run-out distance because the full mass does not spread as quickly as a small part of it. Spreading reduces the flow depth, which is important in many rheologies and bed friction laws, including visco-plastic and plastic rheologies and the Voellmy friction law.

   It may be possible to set the model up so that it actually computes the retrogression, as in Kvalstad's wedge and horst model or in a corresponding simulation with ANSYS-CFX by Gauer. The question of how to integrate such a mechanism in a flow model requires more study. In a first step, however, it might be sufficient that the user of the model can prescribe the sizes of the chunks and the timing of their release.

2. *Multi-layer modeling:* Nearly all quick-clay slides involve a substantial amount of non-sensitive or less sensitive clay, typically located above or downstream of the quick-clay pocket. In Rissa, the layer was thick and strong enough to be rafted more or less intact for several hundred meters, and remnants of flakes A and B have been identified on the lake bottom by means of swath bathymetry.

   The key effect of such a quasi-rigid layer riding on top of the rapidly sheared quick-clay layer is that the shear stress remains above the yield strength throughout the quick-clay layer even if it is thin. In this way, the quick clay acts as a lubricating layer for the flake on top that may attain high velocity and long run-out in this way. Some experimental confirmation of this effect can be found in (Khaldoun et al., 2009), even though it is not as easily understood in their setting, which only involves quick clay.

   The best form of including this effect in the mathematical model remains to be determined. One option is to treat the slide as a train of rigid slabs sliding over quick clay, possibly with the option of letting slabs break if the stress on them exceeds some threshold. The other alternative is to set up a stratified fluid model with different rheologies in the two layers.

3. *Modeling of remolding:* It is anticipated that a critical issue in many hazard assessments involving potential quick-clay slides is whether a slope failure will develop into a slide or not. This problem is discussed extensively by L'Heureux (2012b), making use both of observations collected in

a database and geotechnical and rheological considerations. The energy required for remolding sensitive clay to a certain degree and the ratio of remolding energy and potential energy are the central notions in this context. A question that requires intensive study is the efficiency of sliding in remolding the quick-clay layer partially or completely.

A first step towards accounting for this effect was taken by De Blasio et al. (2003), who heuristically assumed an exponential softening effect depending on the shear accumulated in the shear layer of a Bingham fluid. Using experimental information on the remolding of sensitive clays and differentiating between sublayers in the quick-clay layers, it appears feasible to improve this approach and give it a solid mechanical basis. As L'Heureux (2012b) points out, however, further laboratory testing of Norwegian sensitive clays is necessary.

4. *Buoyancy and hydrodynamic drag:* It is anticipated that a substantial fraction of potential applications of the model involve subaqueous flow, possibly following a phase of subaerial movement. In the simulations presented in this report, the problem was solved by modifying the terrain model so as to include the buoyancy effect. Hydrodynamic drag is easily seen to have a decisive effect on the velocity of all except the slowest subaqueous landslides. A detailed inclusion of this effect is not so simple and computationally expensive, but the simple approximation proposed by the De Blasio et al. (2004) goes a long way towards making the simulated velocities realistic.

Buying or developing in-house? Semi-commercial models like RAMMS—applied to the Byneset slide by Nigussie (Thakur and Degago, 2012)—or DAN3D are much more economical and timelier than a dedicated development in-house. However, the source code is not accessible so that developments needed for specific applications depend entirely on the developer. Adaptation of such a model to quick-clay slides is precisely such a situation. According to the preliminary results presented in this report, neither of the tested models can be recommended for use in consulting work. Unless some other model not available to the authors is shown to solve the encountered problems, there is no realistic alternative to developing a dedicated new model.

However, open-source models such as BING and MassMov2D offer the possibility of developing incrementally. An asset of both these models that is not to be underestimated is their user-friendly graphical interface that allows easy and efficient pre- and post-processing. Developing such an interface is often more time-consuming than coding and debugging the computational kernel. In the case of BING, the code basis in MS VisualBasic™ would have to be ported to a non-obsolete programming language and widget set; also, the numerical scheme requires further development in order to tame the numerical instabilities that plague the model. A thorough scrutiny of MassMov2D and similar codes in view of their adaptability to a quick-clay slide model has to be left to future development work.

6 Acknowledgements

Funding of the preparation of this report by a grant from the joint project NIFS (Naturfare, Infrastruktur, Flom og Skred) of the Norwegian Road Authorities (Statens Vegvesenet SVV, Veidirektoratet), the Norwegian National Rail Administration (Jernbaneverket JBV), and the Norwegian Water Resources and Energy Directorate (Norges vassdrags- og energidirektorat NVE), and by NGI's general research grant from the Research Council of Norway is gratefully acknowledged. Vikas Thakur (SVV, topic leader for sensitive clays within NIFS) and Vidar Gjelsvik (project leader of NGI's topical project on sensitive clays) are thanked for their interest in this project on run-out modelling and their administrative and scientific input. The code of DAN3D has kindly been provided for research purposes by Prof. Oldrich Hungr, University of British Columbia, Vancouver. Vikas Thakur provided digital terrain models and further data on the Byneset slide. D.I. wishes to thank Jon Otto Fossum, Dept. of Physics, NTNU Trondheim for his detailed and most useful explanations of many points concerning the paper by Khaldoun et al. (2009). V.V. acknowledges the warm hospitality and cheerful atmosphere of the International Centre for Geohazards during her stay in Oslo. The authors very much appreciate the many helpful and enjoyable discussions they have had with their colleagues at NGI, most notably Kjell Karlsrud, who in addition provided quality control, and Jean-Sébastien L'Heureux, whose report, papers and direct input on quick-clay slides in general and on the Rissa and Finneidfjord events in particular were invaluable.

7 References

Beguería, S., van Asch, Th. W. J., Malet, J.-P., and Grondahl, S. (2009). A GIS-based numerical model for simulating the kinematics of mud and debris flows over complex terrain. *Nat. Haz. Earth Syst. Sci.* **9**, 1897–1909.

Best, A. I., Clayton, C. R. I., Longva, O., and Szuman, M. (2003). The role of free gas in the activation of submarine slides in Finneidfjord. *In:* Locat, J., and Mienert, J. (eds.), *Submarine Mass Movements and Their Consequences.* Kluwer Academic, Dordrecht, Netherlands, pp. 491–498.

Cepeda, J. M. (2008). The 2005 Tate's Cairn debris flow: back-analysis, forward predictions and a sensitivity analysis. *In:* Proceedings of the 2007 International Forum on Landslide Disaster Management, Hong Kong 2007. Vol. 2, pp. 813–833.

De Blasio, F. V., Issler, D., Harbitz, C. B., Ilstad, T., Bryn, P., Lien, R., and Løvholt, F. (2003). Dynamics, velocity and run-out of the giant Storegga slide. *In:* Locat, J., and Mineret, J. (eds.), *Submarine Mass Movements and Their Consequences.* Kluwer Academic, Dordrecht, The Netherlands, pp. 223–230.

De Blasio, F. V., Elverhøi, A., Issler, D., Harbitz, C. B., Bryn, P., and Lien, R. (2004). Flow models of natural debris flows originating from overconsolidated clay materials. *Mar. Geol.* **213**, 439–455.

De Blasio, F. V., Elverhøi, A., Issler, D., Harbitz, C. B., Bryn, P., and Lien, R. (2005). On the dynamics of subaqueous clay-rich gravity mass flows—the giant Storegga slide, Norway. *Marine Petrol. Geol.* **22**, 179–186.

Furseth, A. (2006). Skredulykker i Norge. Oslo, Norway, Tun Forlag.

Gauer, P., and Cepeda, J. M. (2007). Evaluation of existing numerical models for gravity mass flows. Norwegian Geotechnical Institute, Oslo, Norway. NGI Report 20071268-1.

Gregersen, O. (1981). The Quick Clay Landslide in Rissa, Norway. Contribution to the Tenth International Conference on Soil Mechanics and Foundation Engineering, Stockholm, Sweden, 15-19 June 1981. Norwegian Geotechnical Institute, Oslo, Norway. Publication No. 135, pp. 421–426.

Hungr, O. (1995). A model for the run-out analysis of rapid flow slides, debris flows and avalanches. *Can. Geotech. J.* **32,** 610–623.

Ilstad, T., De Blasio, F. V., Elverhøi, A., Harbitz, C. B., Engvik, L., Longva, O., and Marr, J. G. (2004). On the frontal dynamics and morphology of submarine debris flows. *Mar. Geol.* **213**, 481–497.

Imran, J., Harff, P., and Parker, G. (2001). A numerical model of submarine debris flow with graphical user interface. *Comp. Geosci.* **274**, 717–729.

Janbu, N. (1996). Raset I Finneidfjord – 20. Juni 1996. Unpublished expert's report prepared for the County Sheriff of Nordland, Norway. Report no. 1, rev. 1. Not available to the authors, but cited by (Longva et al., 2003).

Karlsrud, K., Aas, G., and Gregersen, O. (1984). Can we predict landslide hazards in soft sensitive clays? Summary of Norwegian practice and experiences. *In:* Proceedings of the 4th International Symposium on Landslides, Toronto, Ontario, 16–21 September 1984. University of Toronto Press, Toronto, Ontario. Vol. 1, pp. 107–130.

Khaldoun, A., Moller, P., Fall, A., Wegdam, G., De Leeuw, B., Méheust, Y., Fossum, J. O. and Bonn, D. (2009). Quick clay and landslides of clayey soil. *Phys. Rev. Lett.* **103**, 188301.

L'Heureux, J.-S. (2012a). A study of the retrogressive behavior and mobility of Norwegian quick clay landslides. *In:* Proceedings of the 11th International & 2nd North American Symposium on Landslides, Banff, Canada.

L'Heureux, J.-S. (2012b). Characterization of historical quick clay landslides and input parameters for Q-Bing. Norwegian Geotechnical Institute, Oslo, Norway. NGI Report 20120753-02-R.

L'Heureux, J.-S., Eilertsen, R. S., Glimstad, S., Issler, D., Solberg, I.-L., and Harbitz, C. B. (2012a). The 1978 quick clay landslide at Rissa, mid-Norway: subaqueous morphology and tsunami simulations. *In:* Y. Yamada et al. (eds.), *Submarine Mass Movements and Their Consequences*, Advances in Natural and Technological Hazards Research 31, Springer Science+Business Media B.V., pp. 507–516.

L'Heureux, J.-S., Longva, O., Steiner, A., Hansen, L., Vardy, M. E., Vanneste, M., Haflidason, H., Brendryen, J., Kvalstad, T. J., Forsberg, C. F., Chand, S., and Kopf, A. (2012b). Identification of weak layers and their role for the stability of slopes at Finneidfjord, northern Norway. *In:* Y. Yamada et al. (eds.), *Submarine Mass Movements and Their Consequences*, Advances in Natural and Technological Hazards Research 31, Springer Science+Business Media B.V., pp. 321–330.

Longva, O., Janbu, N., Blikra, L. H. and Bøe, R. (2003). The 1996 Finneidfjord slide: seafloor failure and slide dynamics. *In:* Locat, J., and Mienert, J. (eds.), *Submarine Mass Movements and Their Consequences*. Kluwer Academic, Dordrecht, Netherlands, pp. 531–538.

Locat, J., and Demers, D. (1988). Viscosity, yield stress, remolded strength and liquidity index relationships for sensitive clays. *Can. Geotech. J.* **25**, 799–806.

Lyche, E. (2012). Kvikkleireskredet ved Esp på Byneset i 2012. Talk presented at the Quick Clay Workshop, during the meeting Teknologidagene, Trondheim, Norway, October 10–11, 2012. Last downloaded from http://www.vegvesen.-no/_attachment/389134/binary/666860 on 2012-11-20.

McDougall, S., and Hungr, O., (2004). A model for the analysis of rapid landslide motion across three-dimensional terrain. *Can. Geotech. J.* **41**, 1084–1097.

McDougall, S., and Hungr, O., (2005). Dynamic modeling of entrainment in rapid landslides. *Can. Geotech. J.* **42**, 1437–1448.

McDougall, S. (2006). A new continuum dynamic model for the analysis of extremely rapid landslide motion across complex 3D terrain. PhD thesis, University of British Columbia, Vancouver, Canada.

Monaghan, J. J. (1992). Smootheed Particle Hydrodynamics. *Annu. Rev. Astron. Astrophys.* **30**, 543–574.

Natterøy, A. (2011). Skredkatalog om kvikkleire. Presentasjon av det førebels resultatet i katalogen og utgreiing om typiske kjennetegn ved kvikkleireskred. Project thesis, Institutt for geologi og bergteknikk, Norwegian University of Technology and Science (NTNU), Trondheim, Norway. (In Norwegian)

Norsk Geoteknisk Forening (NGF), (1974): Retningslinjer for presentasjon av geotekniske undersøkelser. Oslo, Norway, 16 pp. (In Norwegian)

NVE (2012). Kvikkleireskred ved Esp, Byneset I Trondheim. Norwegian Water and Energy Directorate (NVE), Oslo, Norway. NVE Report no. 1-2012 preliminary version 2012-01-09, 79 pp.

Quan Luna, B. (2008). Benchmarking of debris flow runout distance: Simulation of Frank Slide and Shum Wan Road landslide. International Centre for Geohazards and Norwegian Geotechnical Institute, Oslo, Norway. ICG Report 2008-7-1, 80 pp.

Quan Luna, B. (2012). Dynamic numerical run-out modeling for quantitative landslide risk assessment. PhD dissertation, University of Twente, The Netherlands. http://www.itc.nl/library/papers_2012/phd/quan.pdf (accessed on 28 November 2012).

Rosenqvist, I. T. (1953). Considerations on the sensitivity of Norwegian clays. *Geotechnique* **3**, 195–200.

Rosenqvist, I. T. (1966). The Norwegian research into the development of quick clay – a review. *Engin. Geol.* **1**, 445–450.

Thakur, V., and Degago, S. A. (2012). Utbredelse av skred I områder med sensitive leire. *In:* Thakur, V. (ed.), *En nasjonal satsing på sikkerhet i kvikkleireområder. Proceedings of a workshop at Teknologidagene, Trondheim October 10 and 11, 2012.* Norwegian Water and Energy Directorate (NVE), Oslo, Norway. NVE Report no. 33-2012, 161 pp.

Walberg, Ø. (1993). Verdalsboka. Ras i Verdal, vols. A and B. Verdal municipality, Norway. (In Norwegian)

Kontroll- og referanseside/
Review and reference page

Dokumentinformasjon/*Document information*	
Dokumenttittel/*Document title* Back-analyses of run-out for Norwegian quick-clay landslides	**Dokument nr./*Document No.*** 20120753-01-R
Dokumenttype/*Type of document* Report	**Distribusjon/*Distribution*** Unlimited
	Dato/*Date* 30 November 2012
	Rev.nr.&dato/*Rev.No&date.* 0
Oppdragsgiver/*Client* NIFS-partnere: Statens Vegvesen, Vegdirektoratet v/Vikas Thakur; Jernbaneverkeet; Norges Vassdrags- og Energidirektoratet	
Emneord/*Keywords* Quick-clay slides, Rissa, Finneidfjord, Byneset, runout, velocity, numerical simulation, back-calculation, BING, DAN3D, MassMov2D	

Stedfesting/*Geographical information*	
Land, fylke/*Country, County* —	**Havområde/*Offshore area*** —
Kommune/*Municipality* —	**Feltnavn/*Field name*** —
Sted/*Location* —	**Sted/*Location*** —
Kartblad/*Map* —	**Felt, blokknr./*Field, Block No.*** —
UTM-koordinater/*UTM-coordinates* —	

Dokumentkontroll/*Document control*

Kvalitetssikring i henhold til/*Quality assurance according to* NS-EN ISO9001

Rev./ *Rev.*	**Revisjonsgrunnlag/*Reason for revision***	**Egen-kontroll/ *Self review* av/*by:***		**Sidemanns-kontroll/ *Colleague review* av/*by:***		**Uavhengig kontroll/ *Independent review* av/*by*:**		**Tverrfaglig kontroll/ *Inter-disciplinary review* av/*by:***	
0	Original document	DI		KK		JMC			
		JMC				DI			

Dokument godkjent for utsendelse/ *Document approved for release*	**Dato/*Date***	**Sign. Prosjektleder/*Project Manager***
	30 November 2012	Dieter Issler

NGI (Norges Geotekniske Institutt) er et internasjonalt ledende senter for forskning og rådgivning innen geofagene. Vi utvikler optimale løsninger for samfunnet, og tilbyr ekspertise om jord, berg og snø og deres påvirkning på miljøet, konstruksjoner og anlegg.

Vi arbeider i følgende markeder: olje,gass og energi, bygg, anlegg og samferdsel, naturskade og miljøteknologi. NGI er en privat stiftelse med kontor og laboratorier i Oslo, avdelingskontor i Trondheim og datterselskap i Houston, Texas, USA.

NGI ble utnevnt til "Senter for fremragende forskning" (SFF) i 2002 og leder "International Centre for Geohazards" (ICG).

www.ngi.no

NGI (Norwegian Geotechnical Institute) is a leading international centre for research and consulting in the geosciences. NGI develops optimum solutions for society, and offers expertise on the behaviour of soil, rock and snow and their interaction with the natural and built environment.

NGI works within the oil, gas and energy, building and construction, transportation, natural hazards and environment sectors. NGI is a private foundation with office and laboratory in Oslo, branch office in Trondheim and daughter company in Houston, Texas, USA.

NGI was awarded Centre of Excellence status in 2002 and leads the International Centre for Geohazards (ICG).

www.ngi.no

Hovedkontor/Main office:
PO Box 3930 Ullevål Stadion
NO-0806 Oslo
Norway

Besøksadresse/Street address:
Sognsveien 72, NO-0855 Oslo

Avd Trondheim/Trondheim office:
PO Box 1230 Sluppen
NO-7462 Trondheim
Norway

Besøksadresse/Street address:
Pirsenteret, Havnegata 9, NO-7010 Trondheim

T: (+47) 22 02 30 00
F: (+47) 22 23 04 48

ngi@ngi.no
www.ngi.no

Kontonr 5096 05 01281/IBAN NO26 5096 0501 281
Org. nr/Company No.: 958 254 318 MVA

BSI EN ISO 9001
Sertifisert av/Certified by BSI, Reg. No. FS 32989

Denne serien utgis av Norges vassdrags- og energidirektorat (NVE)

Utgitt i Rapportserien i 2013

Nr. 1 Roller i det nasjonale arbeidet med håndtering av naturfarer for tre samarbeidende direktorat
Nr. 2 Norwegian Hydrological Reference Dataset for Climate Change Studies. Anne K. Fleig (Ed.)
Nr. 3 Anlegging av regnbed. En billedkavalkade over 4 anlagte regnbed
Nr. 4 Faresonekart skred Odda kommune
Nr. 5 Faresonekart skred Årdal kommune
Nr. 6 Sammenfatning av planlagte investeringer i sentral- og regionalnettet for perioden 2012-2021
Nr. 7 Vandringshindere i Gaula, Namsen og Stjørdalselva
Nr. 8 Kvartalsrapport for kraftmarknaden. Ellen Skaansar (red.)
Nr. 9 Energibruk i kontorbygg – trender og drivere
Nr. 10 Flomsonekart Delprosjekt Levanger. Kjartan Orvedal, Julio Pereira
Nr. 11 Årsrapport for tilsyn 2012
Nr. 12 Report from field trip, Ethiopia. Preparation for ADCP testing (14-21.08.2012)
Nr. 13 Vindkraft - produksjon i 2012
Nr. 14 Statistikk over nettleie i regional- og distribusjonsnettet 2013. Inger Sætrang
Nr. 15 Klimatilpasning i energiforsyningen- status 2012. Hvor står vi nå?
Nr. 16 Energy consumption 2012. Household energy consumption
Nr. 17 Bioenergipotensialet i industrielt avfall
Nr. 18 Utvikling i nøkkeltall for strømnettselskapene
Nr. 19 NVEs årsmelding
Nr. 20 Oversikt over vedtak og utvalgte saker. Tariffer og vilkår for overføring av kraft i 2012
Nr. 21 Naturfareprosjektet: Delprosjekt Kvikkleire. Utstrekning og utløpsdistanse for kvikkleireskred basert på katalog over skredhendelser i Norge
Nr. 22 Naturfareprosjektet: Delprosjekt Kvikkleire. Forebyggende kartlegging mot skred langs strandsonen i Norge Oppsummering av erfaring og anbefalinger
Nr. 23 Naturfareprosjektet: Delprosjekt Kvikkleire. Nasjonal database for grunnundersøkelser (NADAG) – forundersøkelse
Nr. 24 Flom og skred i Troms juli 2012. Inger Karin Engen, Graziella Devoli, Knut A. Hoseth, Lars-Evan Pettersson
Nr. 25 Capacity Building in Hydrological Services. ADCP and Pressure Sensor Training Ministry of Water and Energy, Ethiopia 20th – 28th February 2013
Nr. 26 Naturfareprosjektet: Delprosjekt Kvikkleire. Vurdering av kartleggingsgrunnlaget for kvikkleire i strandsonen
Nr. 27 Kvartalsrapport for kraftmarknaden. Ellen Skaansar (red.)
Nr. 28 Flomberegninger for Fedaelva, Kvinesdal kommune, Vest-Agder (025.3A1) Per Alve Glad
Nr. 29 Beregning av energitilsig basert på HBV-modeller. Erik Holmquist
Nr. 30 De ustabile fjellsidene i Stampa – Flåm, Aurland kommune Sammenstilling, scenario, risiko og anbefalinger. Lars Harald Blikra
Nr. 31 Naturfareprosjektet: Delprosjekt 4 Overvåking og varsling Overvåking ved akutte skredhendelser
Nr. 32 Landsomfattende mark- og grunnvannsnett. Drift og formidling 2012. Jonatan Haga
Nr. 33 Naturfareprosjektet: Delprosjekt 6 Kvikkleire. Saltdiffusjon som grunnforsterking i kvikkleire
Nr. 34 Kostnadseffektivitet i distribusjonsnettet – En studie av referentene i kostnadsnormmodellen
Nr. 35 The unstable phyllitic rocks in Stampa – Flåm, western Norway Compilation, scenarios, risk and recommendations. Lars Harald Blikra
Nr. 36 Flaumsonekart Delprosjekt Årdal i Sogn. Siss-May Edvardsen, Camilla Roald
Nr. 37 Naturfareprosjektet: Delprosjekt 6 Kvikkleire. Skånsomme installasjonsmetoder for kalksementpeler og bruk av slurry
Nr. 38 Naturfareprosjektet: Delprosjekt 6 Kvikkleire. Karakterisering av historiske kvikkleireskred og input parametere for Q-BING
Nr. 39 Naturfareprosjektet: Delprosjekt 6 Kvikkleire. Natural Hazards project: Work Package 6 - Quick clay Characterization of historical quick clay landslides and input parameters for Q-Bing

Rapportserien i 2013 forts.

Nr. 40 Naturfareprosjektet: Delprosjekt 6 Kvikkleire. Skred ved Døla i Vefsn. Undersøkelse av materialegenskaper

Nr. 41 Naturfareprosjektet: Delprosjekt 6 Kvikkleire. State-of-the-art: Blokkprøver

Nr. 42 Naturfareprosjektet: Delprosjekt 6 Kvikkleire. Innspill til "Nasjonal grunnboringsdatabase (NGD) – forundersøkelse"

Nr. 43 Naturfareprosjektet: Delprosjekt 6 Kvikkleire. Styrkeøkning av rekonsolidert kvikkleire etter skred

Nr. 44 Driften av kraftsystemet 2012. Karstein Brekke (red.)

Nr. 45 Ny forskrift om energimerking av energirelaterte produkter (energimerkeforskriften for produkter) Oppsummering av høringsuttalelser og endelig forskriftstekst

Nr. 46 Natural Hazards project: Work Package 6 - Quick clay. Back-analyses of run-out for Norwegian quick-clay landslides

Norges
vassdrags- og
energidirektorat

Norges vassdrags- og energidirektorat

Middelthunsgate 29
Postboks 5091 Majorstuen
0301 Oslo

Telefon: 09575
Internett: www.nve.no